DEGREE PROJECT, IN MATERIALS SCIENCE AND ENGINEERING, SECOND LEVEL, SWEDEN 2014

How bending affects the ballistic properties of Armox

RICHARD TENGGREN

KTH ROYAL INSTITUTE OF TECHNOLOGY

Abstract

This thesis discusses how bending of Armox 500T and Armox 440T affects the ballistic properties; it also discusses the bending performance of Armox 500T and Armox 440T.

The purpose is to develop new bending recommendations, and to investigate the correlation between bending radius and maintaining ballistic performance and offer more reliable bending recommendations to the Armox customers. The new bending recommendations will satisfy both mechanical and ballistic performance.

To achieve the purpose, bending tests was made, and then the bended specimens were used to investigate the deformation from the bending. The method hardness mapping was used to describe the deformation in the specimen, because of the lack of information of deformation mechanism in martensitic steels.

To test the ballistic properties, V50-tests were made on bended specimens at Åkers Krutbruk Protection AB. The V50-value is the calculated average value from six rounds, with three stops and three penetrations in a span of 40 m/s.

The result from the testing shows that the bending does not have any significantly effect on the ballistic properties on the tested combinations of materials and ammunitions.

The conclusions from the testing results are that the bending does not significantly influence the ballistic properties for the tested materials and ammunitions and the bending recommendations were greatly improved.

Keywords: Bending, Ballistics, Ballistic properties, Armox, Adiabatic shearing, Armour, Armour steel

Table of Contents

List of Figures

List of Tables

Terminology

Summary of acronyms and symbols appear in the report for this thesis.

Acronyms

UTS	Ultimate Tensile Strength
EME	EM Eriksson
API	Armor Piercing Incendiary
FSP	Fragment Simulating Projectile
BHN	Brinell Hardness Number
UHH	Ultra High Hardness
FMJ	Full Metal Jacket

Notation

Symbol	description	Symbol	description
T_m	Melting temperature	a	Width of elastic zone
t	Thickness	σ_y	Yield stress
$F_{b,Rm}$	Bending force according to UTS	α	Bending angle
		β	Angle of bend
F_b $\sigma_{y,}$	Bending force according to yield strength	$\Delta\alpha$	Springback angle
		M_s	Initial bending moment
F_y	Bending force, elastic	M	Bending moment
R	Punch radius	M_{max}	Max bending moment
R_i	Internal bend radius	C	Parameter, function of l/t
W_d	Die width	l	Effective moment arm
L	Work piece width		
R_m	Ultimate tensile strength		
R_e	Yield point		
M_f	Final bending moment		

1. Introduction

1.1 Company information

SSAB is a producer of steel, which include armor steel, used to protect human life. They develop, manufacture and market heavy steel plates in Oxelösund, located south of Stockholm, on the Baltic coast. Armox is one of the armor steels, manufactured by SSAB and is available in hardness range from rolled homogeneous armor steel (280 *BHN*) to ultra-high hardness steel (>650 *BHN*). Armox steels are well known for the high toughness in relation to the hardness. The aim is to offer a high mass efficiency due to the weight, which is a critical factor in many vehicle projects [1] [2].

The production of Armox is based on iron-ore metallurgy through blast furnaces, steel deoxidation in an LD converter. The vacuum treatment, results in very clean steel. Thanks to the modern four-high plate mill it is possible to roll with large reductions, resulting in fine-grained microstructures in Armox. Various heat treatments are used to achieve the desired hardness or toughness requirements [3].

Armox customers are leading manufacturers of protection equipment all over the world. Armox is mainly used to build all kind of armored military vehicles and to armouring of civilian cars and buildings. The use of Armox differs greatly between the customers [1].

1.2 Background

Armox steels are martensitic steels which are made by a specific production process, and ends with rolling, quenching and tempering. This treatment results in excellent mechanical properties of Armox, as high hardness, tensile strength and good toughness. SSAB recommend secondary processing, as cutting, welding and shaping at temperatures lower than 200 °C, due to over tempering and degradation of the excellent mechanical properties in heat affected zones [1].

A common forming process among the Armox customers is air bending. SSAB offers today bending recommendations to their clients which were issued in 1999 and partly upgraded 2012. The purpose of these recommendations is to inform the customers about the mechanical limits of the material [4].

The current recommendations are not up to date and SSAB know it should be possible to bend Armox with smaller radius due to improved production. SSAB will also, if possible, make recommendations for bending while maintaining ballistic performance. Today SSAB recommend a bending radius of five times the thickness for Armox 500T with thickness up to 8 mm and six times for plate thicknesses of 8-15 mm [5].

When manufacturing ballistic protected applications it is very important to have good cold forming properties as every weld has a negative effect on the ballistic properties. To avoid this, the cold forming is the best option [4].

1.3 Purpose

The purpose of this project is to develop new bending recommendations, investigate the correlation between bending radius and ballistic performance; this also includes explaining the altered microstructure to the ballistic results, due to the bending. SSAB would like to offer better and more reliable bending recommendations to the customers without affecting the ballistic properties.

1.4 Methods

In order to investigate how bending affect the ballistic performance of Armox, bending and ballistic tests, as well as metallographic examinations, will be carried out.

In addition to these tests a literature study will be performed to achieve an understanding of the underlying causes of the later results.

2. Theory – Plastic forming

2.1 Plastic forming

The definition of plastic forming implies that by plastic deformation transform the metal's shape while maintaining the same volume and mass. Sheet metal is usually formed in cold state at a maximum temperature of 0.3 x T_m. Hot forming of sheet metal is done in a minimum temperature of 0.6 x Tm. The benefits with the hot state forming are that the material will recrystallize and are easier to form, the disadvantages is that the surface will not be as good as in the cold state. Cold state forming will result in higher strength than the hot state [6].

When a metallic material is plastically deformed the concentration of dislocations will increase, result in an increased hardness, known as work hardening. Dislocations represent an additional contribution to the systems energy. Since the nature strive towards a state of lowest energy (actually the free energy at a constant external pressure and temperature), it can be expected that dislocations can be lost spontaneously from the material. This also occurs to some extent if the temperature is raised sufficiently to increase the atomic mobility. When dislocations become more mobile than at room temperature, they arrange themselves with respect to each other and any internal stresses in the material [7].

Work hardening contributes to increasing the need of force and wearing of the tool [6].

2.2 Bending

Bending is a plastic processing method in which the sheet metal is mainly formed by a bending moment. The method is used to give the sheet metal a curved shape. Air bending in v-die is the most applied method.

Bending works are usually performed in mechanical or hydraulic press brakes. Edge weighting machines are mostly used for small batches [8].

Bending is one of the most common sheet metal forming processes and includes a few different methods. The most suited method for a detail differs with the final shape and how big batches that is required. The different bending methods are; V-die-bending, U-die-bending, free bending, roll forming and roll bending [9]. Only the V-die-bending is relevant to this thesis, and therefore it only deals with V-die-bending.

During bending, a tensile stress on the convex side of the bend occurs while on the same time it becomes compressive stresses on the concave side. The tensile stress increases as the bending radius decreases. Bendability of a material is normally defined by the minimum bending radius for use without rupture occurs.

Spring back is caused by elastic strains and it will increase with increased yield strength, work hardening and die width. The yield strength has the biggest effect on the spring

back. In order to bypass springback during bending it is common to use over bending to compensate for the springback [8].

2.2.1 Bending forces

The fundamental of bending is that the yield point of the material must be exceeded for plastic bending to occur. During bending a tensile stress occurs on the convex side of the bend while on the same time it becomes compressive stresses on the concave side, as shown in Figure 1 [9].

This is similar to the deflection of a beam under load [10].

Between the convex and concave sides, the neutral axis of the material is located, there the stresses are zero. When the yield point is exceeded, the material start to work hardening, while on the same time a plastic zone start to grow towards the neutral axis from both convex and concave side of the bend. The material is still elastic around the neutral axis and the size of the elastic zone determines how much springback there will be after bending. If the bending results in plasticization of the material, this means that the springback will be minimized [9].

If the bending results in failure or fracture, this will occur at the convex side of the bend surface [10].

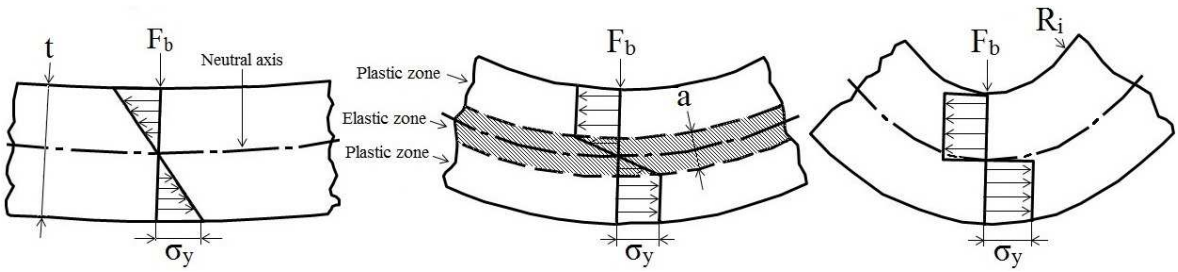

Figure 1. The three different sequences and stress distributions during bending.

According to Figure 2 below, the bending force, F_b, will vary with the punch depth. Initially the bending force grows linearly up to the material's yield strength, σ_y, and then the plastic deformation and work hardening occur. During the initial phase of bottom

bending the bending force increases very quickly as shown in Figure 2 [9].

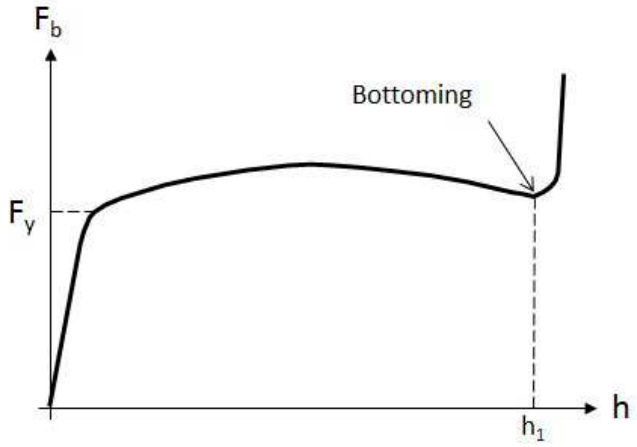

Figure 2. The bending force as a function of the punch depth.

In the initial stage of bending the bending moment, M_s (Initial bending moment), can be defined by Equation 1 up to the beginning of the plastic phase [9].

$$\boldsymbol{M_s = \sigma_y \cdot W} \quad (1)$$

$$\boldsymbol{W = \frac{L \cdot t^2}{6}} \quad (2)$$

$$\boldsymbol{M_s = \frac{\sigma_y \cdot L \cdot t^2}{6}} \quad (3)$$

W is the bending resistance for a rectangular section of width L and the thickness t, corresponding to the length and thickness of the plate. As mentioned above the Equation 1, it only applies to the beginning of the bending sequence, up to the yield point. When the plastic zone begins to develop, a new equation is needed for describe this, as shown in Equation 4. The width of the elastic zone is symbolized by a [9].

$$\boldsymbol{M = \sigma_y \left(\frac{La^2}{6} + \frac{L(t^2 - a^2)}{4} \right) = \sigma_y \frac{L(3t^2 - a^2)}{12}} \quad (4)$$

In the end of the bending sequence, the plastic zone extends into the neutral axis and the elastic zone will disappear. This leads to Equation 5 as shown below, M_f symbolizing final bending moment [9].

$$\boldsymbol{M_f = \frac{\sigma_y \cdot L \cdot t^2}{4}} \quad (5)$$

The moment distribution during the bending sequence of V-die bending is shown in Figure 3. The bending force, F_b, is opposed by two reaction forces at each edge of the V-die, $F_b/2$. The movement between the die and the sheet are resulting in frictional forces at each corner of the die. Frictional forces can be described as $\mu(F_b/2)$ and does not affect the moment distribution [9].

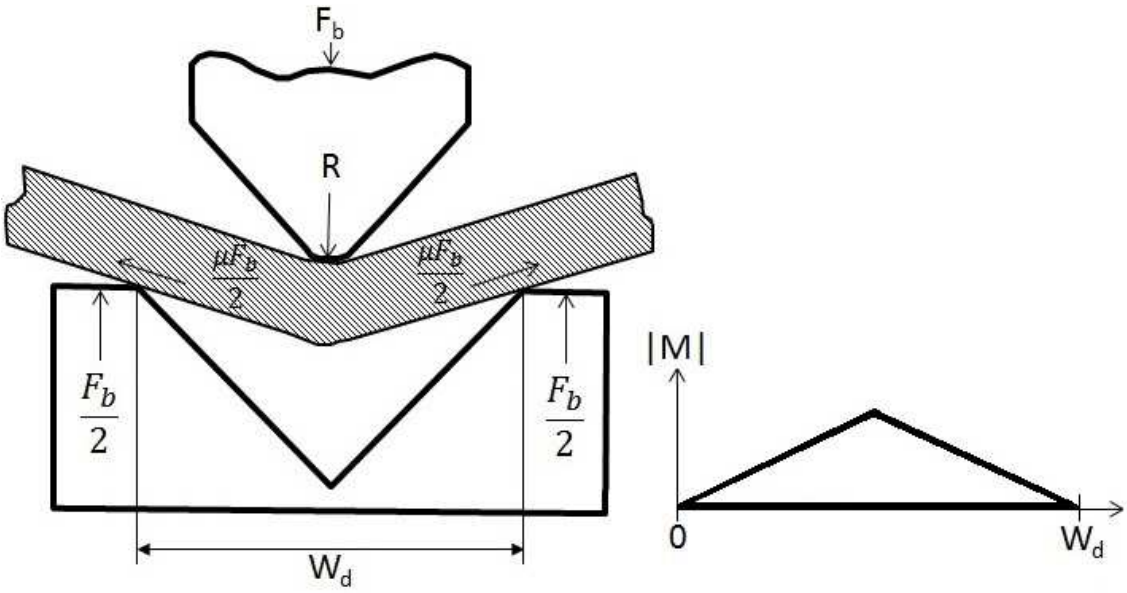

Figure 3. The moment distribution.

The bending moment is greatest underneath the punch. The maximum moment occurs at the end of the bending sequence and can be described as in Equation 6, and W_d symbolizing the width of the die [9].

$$\boldsymbol{M_{max} = \frac{F_b \cdot W_d}{4}} \quad \textbf{(6)}$$

Equation 5 and Equation 6 now provides a relation for bending force, F_B, as described in Equation 7 [9].

$$\boldsymbol{F_{b,\sigma_y} = \frac{L \cdot t^2 \cdot \sigma_y}{W_d}} \quad \textbf{(7)}$$

The bending force can also be expressed so that it depends on the material's ultimate tensile strength instead of the yield strength, as describe in Equation 8 [9].

$$\boldsymbol{F_{b,R_m} = \frac{L \cdot t^2 \cdot R_m}{W_d}} \quad \textbf{(8)}$$

The equations above include a number of approximations; the first one is that the neutral axis is assumed to remain at the same position during the bending, which is not always the case. In the end of the bending sequence, when the deformation becomes fully plastic the neutral axis will be displaced towards the concave side of the bend. This is an effect when the extension of the material on the convex side of the bend is greater than compression on the concave side. This is due to frictional forces between the die edge and the sheet, also the thickness of the material affects. The second approximation is that none consideration of the work hardening have been done, an elastic-ideal plastic material. This means that the Equation 4, Equation 5 and Equation 7 only will be valid for materials without work hardening. When the work hardening is considered, the stress distribution in the bend will be as shown in Figure 4 below [9].

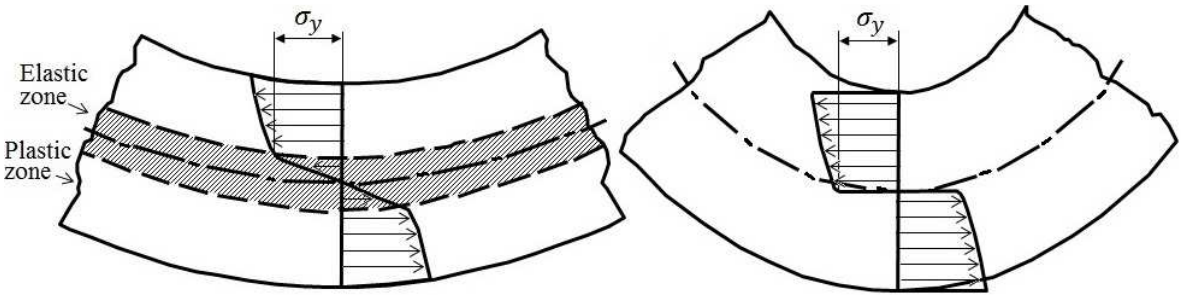

Figure 4. Stress distribution in the bend, to left the elastic-plastic and to right the plastic phase, in consideration to work hardening.

The bending force depends on the inversely ratio between the die width and the square of the sheet thickness, W_d/t^2, when the ratio decrease the force will increase. If the average values of yield point and UTS are used in the expression for bending force, some consideration to work hardening will be done. Equation 9 describes an expression which takes consideration to both the tool geometry and the work hardening [9].

$$F_b = \frac{C \cdot L \cdot t^2}{l} \cdot \frac{R_m + R_e}{2} \qquad (9)$$

F_b = Bending force [N] R_m = UTS [MPa]

L = Bend length [mm] R_e = Yield point [MPa]

t = Workpiece thickness [mm] C = Parameter

l = Effective moment arm [mm]

The parameter C is a function of the effective moment arm and thickness, it is determined through the use of Figure 5 [9].

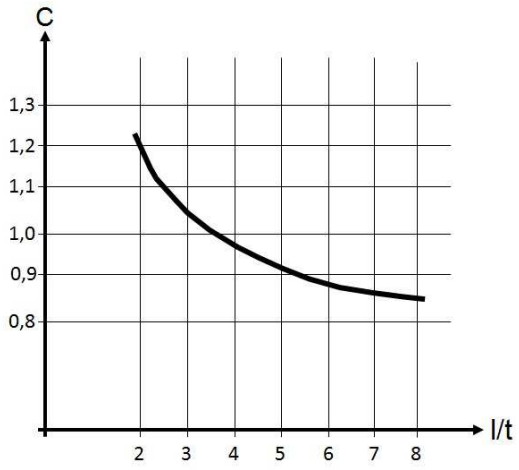

Figure 5. For determining the parameter C.

In Figure 6 the effective moment arm in V-die-bending, l, which is used above in Figure 5 defined [9].

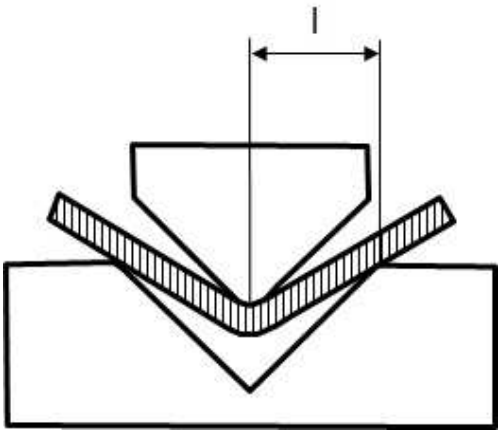

Figure 6. Defines the effective moment arm in V-bending.

The required force is inversely proportional to the half of die width, *l*, this make it possible to increase the die width if the accessible force is to insufficient to make bending possible [9].

2.3 V-die bending

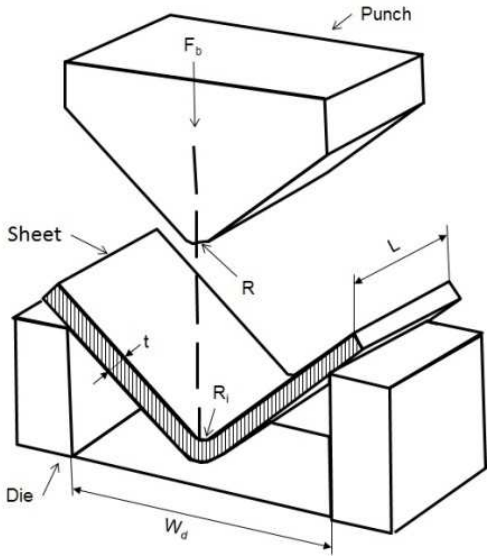

Figure 7. An illustration of V-die bending and a description of the components.

Tool settings for bending angels up to 180˚ can be used in V-die bending. The most common is bending in 90˚ as shown schematic in Figure 7.

Normally the bending is done when the punch push material down into a V-shaped die, as in the schematic Figure 7. The bend of the material when pulled into the tool depend mainly on the ratio between the tool width and the plate thickness.

The punch tip radius should be increased for increased strength of the work material. If the punch radius is too small there is a risk of cracking.

V-die bending can be divided into two types, air bending and bottom bending as shown schematic in Figure 8. Only the air bending is relevant to this thesis, and therefore is bottom bending excluded. Bottom bending appears when the punch forces the material to contact with the die, an initial state of the coining process [9].

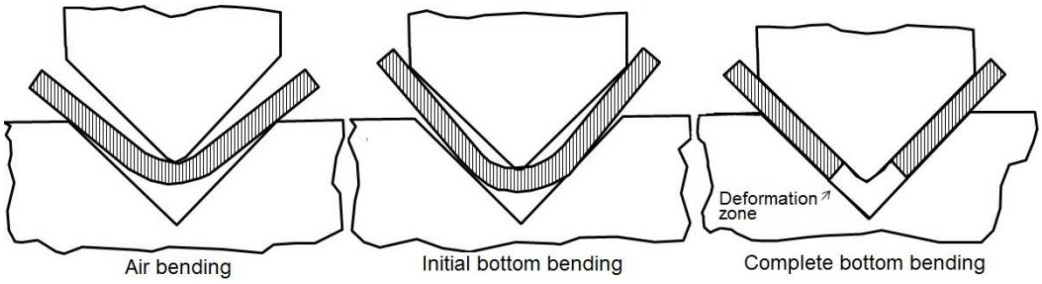

Figure 8. The difference between air bending and bottom bending.

2.3.1 Air bending

When air bending the sheet material is only in contact with the die edge radii and the tool motion is cancelled before the sheet bottoms in the die, hence the name air bending.

When air bending of thinner sheet metal, t<3 mm, the radius of the punch has no effect of the internal radius of the bend. The internal radius of the bend depends of the ratio between the sheet thickness and die width, even the strength of the material depends. When bending of thicker sheet metal, t>3 mm, the internal radius of the bend depends of the punch radius. This is shown in Figure 9.

The bending angle is only controlled by the stroke length at air bending. To compensate for the springback the stroke will be long enough to get the desired bending angle [9]. The punch radius is symbolized by R and the internal bend radius is symbolized by R_i, the radius of the formed material.

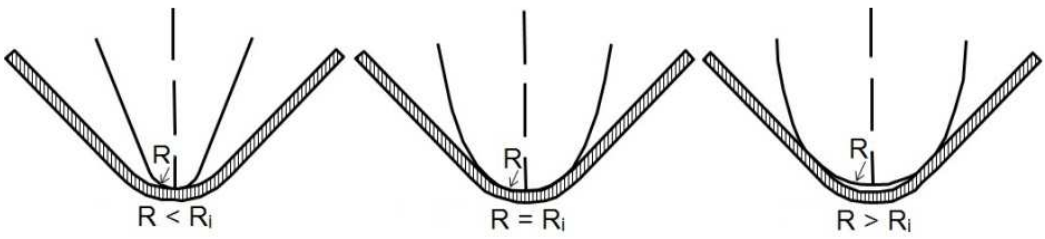

Figure 9. With relatively thin sheets, punch radius has no effect on the shape of the bend. R=punch radius, R_i=internal bend radius on the sheet after unloading.

During bending the sheet metal also thins slightly in the bend area [10].

2.3.2 Springback

During bending, there must always be taken into account that the bent material has springback after unloading. Springback is a material's tendency to partially return to its original shape when the bending force is released. This springback occurs because of the elastic deformation. Together with the internal stresses caused by the bending a residual stress distribution is obtained in the bent material's cross section, as in Figure 10. This residual stress distribution depends on the degree of plastic deformation of the material; it is these residual stresses which causes the springback [9].

To avoid fracture in the bending area, the maximal tensile stress should be less than the UTS [10].

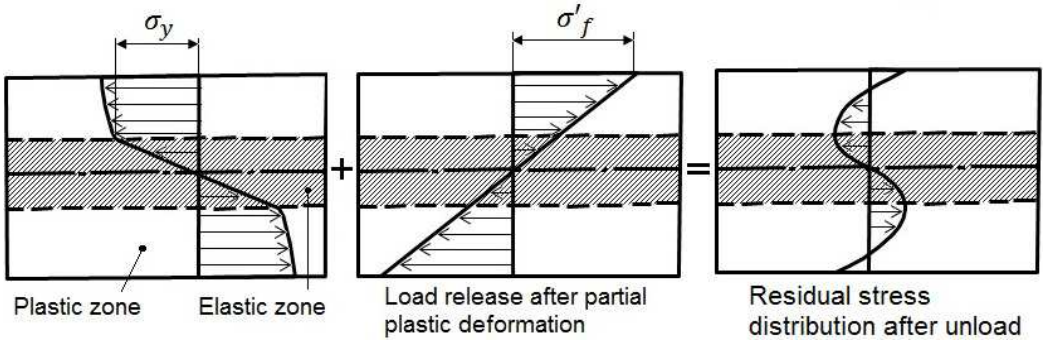

Figure 10. Superposition of stress distribution from bending and load releases gives a residual stress distribution in the cross section.

If the bending results in fully plasticizing, for example by bottom bending, the springback is almost eliminated. The springback increases with the materials strength and die ratio, W_d/t. Material yield point has the greatest effect on the springback. Increased punch radius also gives more springback because of the reduced plastic deformation [9].

To overcome the springback, a certain amount over-bending takes place. There are methods to calculate the size of the over-bend angle in order to compensate for the springback [9].

SSAB has conducted an empirical analysis that resulted in Equation 10 which can be used to roughly describe the over bending angle at air bending to 90˚ and with die width of 10 *t* [9].

$$\Delta\alpha = 0,0143 {R_e}^{0,94} \cdot \left(\frac{R_i}{t}\right)^{0,1} \quad (10)$$

The typical values for springback for Armox are between 10-20 ˚ [4].

3. Theory - Ballistics

3.1 Intro of ballistics

Ballistic is the science of flying objects, the projectile's flight can be divided into three regimes. First up is the interior ballistics, which delivers the projectile into its flight. Then the exterior ballistics comes, which pursues and guides the projectile through its flight. Last out is the terminal ballistics, responsible for the end of the flight. The basic purpose of firing a projectile is to defeat a target [11].

The most common tasks are: to penetrate or perforate the target using the kinetic or chemical energy; fragmenting of the projectile body using its high explosives; blast at the target area delivered by the chemical energy of the explosive cargo; and the dispersal of the cargo for lethal or other missions , like smoke, illumination, propaganda dispersal, etc. [11].

3.2 Penetration and perforation

Penetration is defined as when a projectile creates a discontinuity in the surface of the target. After the projectile or its remnants have been removed, then if light may be seen through the target, perforation has occurred [11].

It is a wide range of impact velocities when projectiles hits metallic targets. Due to the nature of the target material is such that different velocities, somewhat different techniques must be used. Under 250 m/s the penetration can be coupled to the targets overall structural dynamics. The response of the material is approximately 1 ms. When the speed increases further to 500-2000 m/s, the dominated problem is the local behavior of the target and sometimes the penetrator. The size of the affected local zone is about 2-3 times bigger than the projectile diameter from the center of impact.

When a projectile hits a target, compressive waves will propagate into both the target and the projectile. From the lateral free surfaces of the penetrator, relief waves will propagate inwards, cross the centerline and generate a high tensile stress. A two-dimensional stress state will occur if the impact is normal, but if it is oblique, bending stresses will be generated in the penetrator.

When the compressive wave hits the free surface of the target, it will transform to a tensile wave in the target. It is possible that the target will fracture already at this point. If the projectile perforates the target, usually toward the normal of the surface, the projectile may change direction. Targets are categorized into four broad groups because of the differences in target behavior, based on the proximity of the distal surface.

- When there is no influence of distal boundary on penetration; a semi-infinite target.
- When the boundary influences the penetration after the projectile is some distance into the target; a thick target.
- When the boundary exerts influence throughout the thickness; an intermediate thickness target.
- When the stress or deformation gradients are neglible throughout the thickness.

There are several possible methods that may cause the target to fail when subjected to an impact. The most important parameters are the material properties of the target and also the penetrator, the velocity of the impact, the shape of the projectile, the geometry of the supporting structure to the target and also the dimensions of the target and projectile. The different failure modes will be described in Section 3.3 [11].

3.3 Ballistic failure modes

There are several types of failure in ballistic testing, as shown in Figure 11 below. These will now briefly be described.

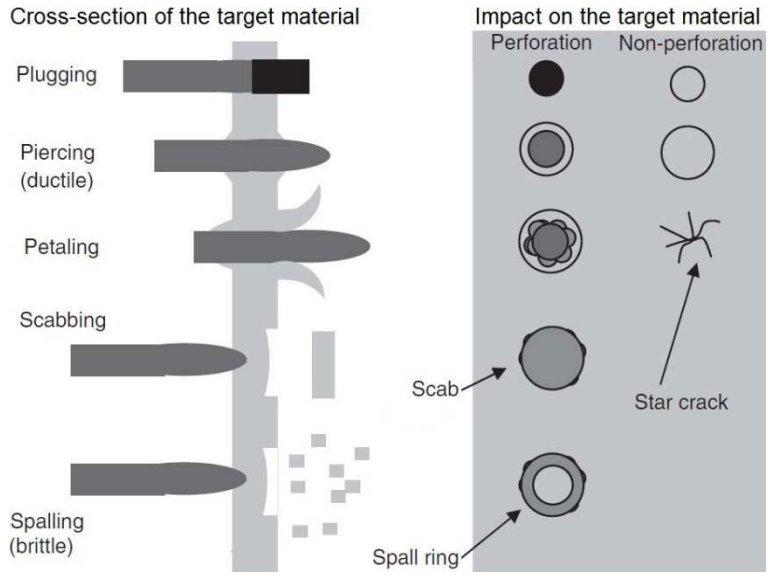

Figure 11. Different failure modes when a projectile hits a target [11].

Plugging is common in relatively ductile materials, and usually when the impact velocity for the projectile is close to the ballistic limit.

Piercing is a phenomenon which can be divided into two phases. Thicker plates are often defeated by this failure mode. The first phase consists of a radial displacement of the target material, and sometimes plugging occurs at this

stage. This phase is followed by plastic flow and yielding of the target material, which can be treated as a fluid during this phase.

When the radial and circumferential stresses are high, petailing is a common failure mode if the projectile impact velocity is close to the ballistic limit.

A similar mode is scabbing, which results from large plate deformation which begins in a crack at a local inhomogeneity. Both of these two modes are brittle, and occur usually in weak and lower density materials. The radial cracking is most common in ceramic materials, because of the tensile strength is lower than the compressive strength, but it also occurs in some steels.

Spalling is the result of wave reflection from the rear side of the target. This failure mode is very common, especially for materials stronger in compression than in tension [11].

3.4 Adiabatic shearing

When a plug is formed under an impact of a target, adiabatic shearing occurs. Initially on impact, a local ring of very intense shear is generated. As this occurs very quickly, in about milliseconds, the target does not have time to build up any motion. Heat is then generated locally in the target. The heat cannot be conducted away because of the large deformation rate and the short time scale. Due to the high temperature, the material properties are weaker at this point and this results in that the material yield readily and flows plastically. The process then continues by itself. Lastly a plug is formed and breaks free from the target. Usually the plug will break up if the perforation velocity is exceeded by about 5-10% over the minimum perforation velocity. If projectiles with blunt noses are used then the tendency for plugging will increase [11].

3.5 Threat standards

Almost every country have their own standard for ballistic protection material, the most common ones use by SSAB and their customers are STANAG 4569 [12] (conducted by NATO) and the EN 1522 [13]/VPAM [14] (UN) [4].

3.5.1 STANAG 4569

NATO has issued the specification, STANAG 4569 [12], Protection Levels for Occupants of Logistics and Light Armored Vehicles. The standard includes threats of small and medium caliber kinetic energy ballistic projectiles and fragment simulating penetrators to simulate artillery bursts.

The standard intends techniques and reproducible test procedures for evaluating the ballistic resistance of vehicle armour components and also the required vehicle vulnerable area assessment.

The threats are segregated into 5 different levels of increasing magnitude of threats, where the level 1 is for mainly intended civilian threats and level 2 and higher are for different level of military threats [12].

3.5.2 EN 1522 / VPAM

EN 1522 [13] defines the requirements and classification that windows, doors, shutters and blinds must be fulfilled when testing in accordance with EN 1523 [15].

This standard is suitable for attacks of handguns, rifles and shotguns on windows, doors, shutters and blinds including the frames and fills, for use in both internal and external locations in buildings. In order to achieve the classification of bullet resistance for blinds and shutters, they must be tested separately and not in conjunction with a window or door [13].

VPAM [14] and EN 1522 [13] are roughly the same standard; EN 1522 is for buildings and structures, while VPAM is for plates and vehicles. VPAM cover a larger amount of threats and ammunitions and can be considered more complete than EN 1522. The customers are usually demanding the EN 1522 instead of VPAM, which they should be asking for. VPAM is newer and have not really had a breakthrough yet, unlike the EN 1522 which have been around for a long time [4].

VPAM was founded in 1999, with the aim to promote experience exchange and mutual assistance with possible questions regarding bullet resistant materials and constructions between the members. Today the association includes the members from six European countries [14].

3.6 Ammunition

Caliber is normally defined as the inner diameter of the barrel, and the projectile diameter is usually 0.2 mm larger than the twisted barrel to achieve rotation of the projectile. In most cases the calibers are named after the barrel dimensions in millimeter or in inches.

A projectile can be built in many different ways, but there are mainly two different types: ordinary ball ammunition (e.g. full metal jacket) or armour piercing ammunition (AP) [4]. The ordinary ball ammunition has a lead or soft steel core normally covered with a jacketing of copper. The armour piercing ammunition also has a core of hardened steel or hard carbides. Both types are illustrated in Figure 12 [4].

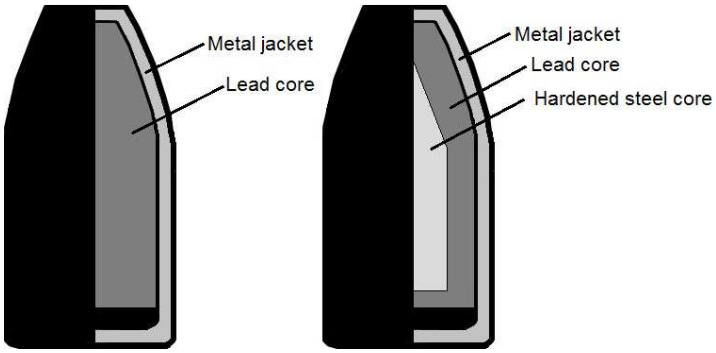

Figure 12. A full metal jacket-bullet to the left and an armour piercing-bullet to the right.

The ammunition corresponding to the standards and threat level in Section 3.5 will be presented and described below in Section 3.6.1 to 3.6.4.

3.6.1 7.62x39 API BZ

This is the standard cartridge for the Russian armed forces. All the American ammunition manufactures offers this cartridge today, brass case, and non-corrosive Boxer primer. Surplus military ammunition occurs from current and former communist countries at low cost, is usually steel cases with corrosive Berdan primers [16].

Previous military cartridges generally were suitable for hunting rounds with proper bullets, but this does not apply to 7.62x39, that do not fit hunting other than for small game. The 7.62x39 are great for military use.

Still the 7.62x39 is definitely a close-range cartridge. The barrel bore diameter is normally .311-inch (7.90 mm) but .308-inch (7.82 mm) diameter bullets can also be used with good results [16].

API stands for Armour-Piercing-Incendiary and BZ is the Russian equivalent of API, and stands for Bronebojno-zazhigatelnaya [4].

3.6.2 Fragment Simulating Projectile

Fragment Simulating Projectile (FSP) is based on a standardized cylindrical projectile with a chisel nose, shown in Figure 13. Available in Caliber .22 Type 1, Caliber .22 Type 2, Caliber .30, Caliber .50 and 20 mm. This projectile is designed to be capable of gun firing to simplify testing of armour [17].

FSP is used to simulate the effect of artillery shells [4].

In Figure 13 below the drawing of the 20 mm fragment simulating projectile are shown.

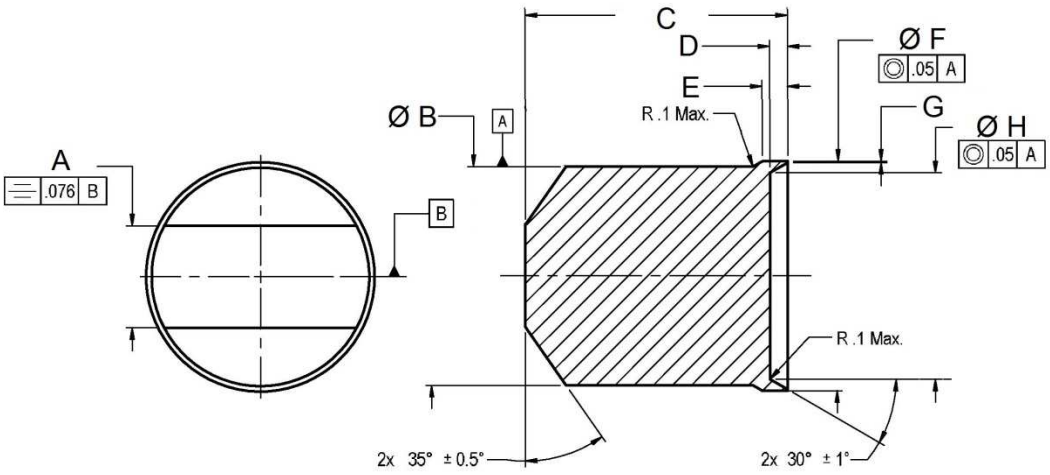

Figure 13. Drawing of the 20 mm fragment simulating projectile.

In Table 1 below the dimensions to the drawing above is shown [17].

Table 1. Dimensions of the 20 mm fragment simulating projectile.

Weight (g)	A (mm)	Ø B (mm)	C (mm)	D (mm)	E (mm)	Ø F (mm)	G (mm)	Ø H (mm)
53.8±0.26	9.27-0.4	19.89±0.05	24.00	1.62±0.05	2.31±0.05	20.83+0.08	0.2 max	18.80±0.12

The FSP´s are used to simulate sharp-edged pieces of steel bomb casings which have a much higher energy than assault rifle bullets [18].

3.6.3 7,62x51 NATO Ball M80

In the 1950´s U.S submitted their new T-65 cartridge for trial in NATO small arms. Basically, it was a shortened 30-06 case with the same caliber bullet and about the same dimension on the case head. Case length was reduced from 63 mm to 51 mm for 7.62 mm T-65. This resulted in a lighter, more compact cartridge and rifle. Some of the other NATO allies provide more advanced entries than the T-65 cartridge. The U.S. used its considerable influence to override all allied objections raised against the 7.62x51 mm NATO cartridge, in order to get it adopted. It is still a NATO standard today. 1957 the U.S. army adopted the M-14 rifle in 7.62x51. The M60 machinegun was also chambered for this cartridge, as are various sniper rifles [16].

During the Vietnam War, the U.S. military adopted the 5.56x45 mm cartridge for their new M-16 rifle, which greatly upset the other NATO allies. At the end of the 70s, a series of NATO tests started which resulted in the 5.56x45 mm cartridge was standardized in 1980. Both the 7.62x51 mm and 5.56x45 mm NATO remain as standard rounds. Recently the chamber infantry assault rifles switched to 5.56x45 mm and leaving the 7.62x51 mm cartridge for the machineguns. Almost all NATO allies manufacture the 7.62x51 mm cartridge, even non-NATO countries and many others also use this cartridge [16].

3.6.4 5.56x45 SS109 (M855)

5.56x45 was originally developed to be used for Armalite AR-15 rifle and was first tested by the U.S. Air Force as a possible replacement for M-1 Carbine in the early 1960s. AR-15 later develop into the selective-fire M-16 that was used by the U.S military in 1964, after several years of testing at the U.S. Continental Army Command at Fort Monroe, Va. The rifle and cartridge was tested for the first time in war in the Vietnam War in the early 60's [16].

In the beginning the 5.56x45 bullet cartridge had a 55 grains (~3.56 g) spitzer boattail bullet with a muzzle velocity of 3250 fps (990.60, m/s). The 5,56x45 bullet was the standard U.S. military cartridge until 1984. In the 80´s the FN-designed 5.56 mm, 62-grain (~4.02 g) SS109 bullet was adopted by NATO. U.S. designated M855 instead of SS109. The new load uses a spitzer boattail bullet with a mild steel penetrator in front of the lead base, and results in a muzzle velocity of 3100 fps (944.88 m/s). To stabilize the longer and heavier bullet for the 5.56 mm rifles, a quicker rifling twist, one turn by every 7 inches (~177.8 mm*)* was needed. This improvement of the bullet resulted in a higher retained velocity and greater accuracy at longer range; the penetration characteristics were also improved [16].

3.7 V_{50} ballistic test

The v_{50} is the velocity at which a given projectile will defeat a given target 50% of the hits. The standard MIL-STD-662F [19] provides general guidelines for procedures, equipment, physical conditions and terminology to determine the ballistic resistance of metallic, non-metallic and composite armor against small arms projectiles. This test procedure determines the v_{50} ballistic limit of armor [19].

The standard is intended to be used for research and development of new armor materials and is applicable to multiple types of armor [19].

The standard has a few limitations, as following:

> *When specified by the procuring activity, ballistic acceptance of armor may be based upon pass/fail or accept/reject criteria other than the V_{50} BL(P) ballistic limit method contained herein.*
>
> *Military activities or DoD contractors may use in-house ballistic test facilities and equipment not covered by this standard (see MIL-STD-1161).*
>
> *This standard does not take precedence over nor supersede armor specification ballistic test procedures.*
>
> *Unique requirements for the ballistic testing of specific end-items not covered in this standard should be specified in the contract* [19].

The v_{50} test uses an electric counter type chronograph to measure the velocity of the projectile. A standard setup is illustrated in the Figure 14 [19].

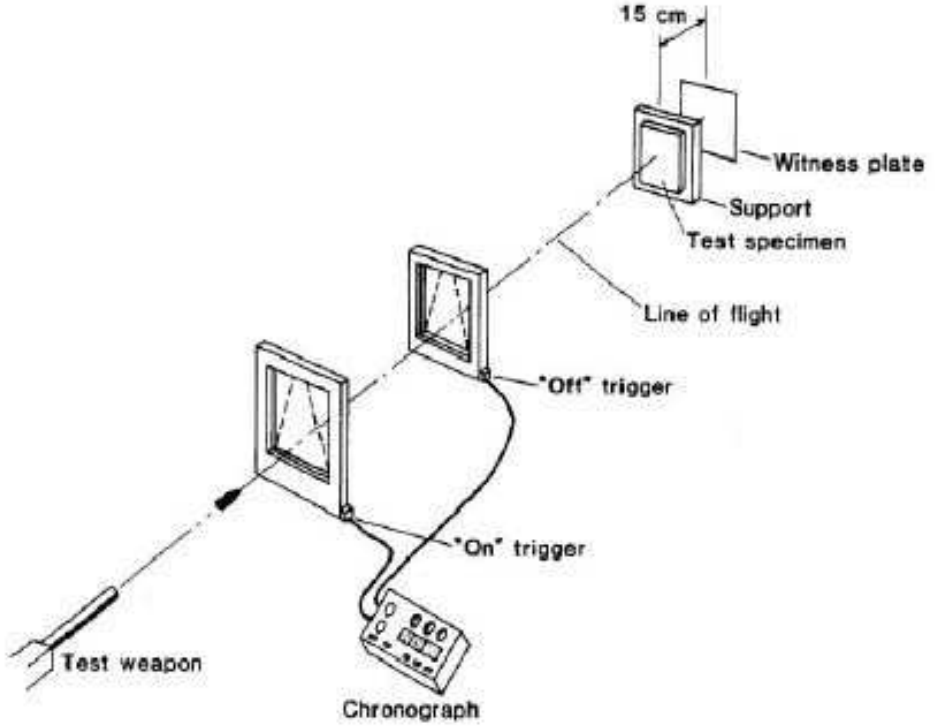

Figure 14. The test rig in a typical v_{50} test [20].

The projectile is fired from the test gun, travels through the first chronograph. Then the timer starts to count the time, then the projectile passes through the second chronograph and the timer stop to count the time, the velocity is then calculated as the distance between the chronographs are known. The projectile hits the target, and possibly shatter penetrates the witness plate behind the target, indicating whether any penetration occurred [20].

3.7.1 Definitions v_{50} test

Some terms that are defined in the standard of v_{50} test are explained below:

A ballistic impact is defined as impacts due to hits on the target by projectiles, fragments or other aerodynamically-affected threat mechanisms [19].

The ballistic limit defined as the minimum or maximum speed for a given projectile, to repeatedly completely or fails to penetrate armor of a given thickness and physical properties at a specified angle of obliquity. It is impossible to control the striking velocity precisely while during firing tests, it also exist a zone of mixed results. The projectile may completely penetrate or only partially penetrate under identical conditions, statistical approaches are necessary, based upon limited firings. The velocity, at which complete penetration and incomplete penetration are equally likely to occur, is in a few

methods approximated to be defined as the v_{50}-point. Another one is the v_0-point that is approximated defined as the velocity at which no complete penetration will occur. The last one is the v_{100}-point that is approximated defined as the minimum velocity at which all projectiles will completely penetrate [19].

The ballistic limit, protection criteria, $v_{50}BL(P)$ is defined as the average of an equal number of highest partial and lowest complete penetration velocities which occur within a specified velocity spread. The normal up-and-down firing procedure is used, if the projectile complete penetrating the target the velocity of the projectile decreases to get a partially penetrating, and vice versa [19].

A 0.51 mm thick 2024T3 sheet of aluminum is placed 152+12.7 mm behind and parallel to the target as a witness plate, to testify of completely penetrations. If the witness plate is completely penetrated, it is considered as a complete penetration also for the target [19].

Two partial and two complete penetration velocities, are normally the minimum number of velocities required to complete the ballistic limit (P). The numbers of rounds are normally four, six or ten for ballistic limits. The size of the velocity span depends on the armor material and test conditions, the maximal velocity span which are normally used is 40 m/s [19].

A fair impact is defined as a hit when an unyawed fragment simulating projectile or test projectile hits an unsupported area, in an area with a specified obliquity and at a distance of at least two projectile diameters from any previous hit, or disturbed area due to an effect, or from any crack or edge of the test specimen [19].

A complete Penetration (CP) occurs when a projectile, any fragment thereof or of the test specimen perforates the witness plate, resulting into a hole or a crack which gets visible in light of a 60-watt, 110-volt bulb placed proximate to the witness plate. Partial penetration (PP) is defined as any incomplete penetration [19].

3.7.2 Performance

The v_{50} velocity is first estimated by a calculation. Then a projectile with an initial velocity, v_s, as close as the estimated velocity possible is fired. Suppose that the speed of this experimental firing ends up a bit above the estimated speed. Assume that shot 1 only resulted in partial penetration, so then the velocity increases greatly to shot 2, then suppose that it now achieved a complete penetration. Assume now that v_{50} is located between shot 1 and 2, fire shot 3 with a velocity halfway between them and it results in a complete penetration. Therefore the velocity need to be further reduced to get a partial penetration, and then increased to get a complete penetration. This procedure

will continue until three complete penetrations and three partial penetrations with the difference between highest and the lowest velocities in the set less than 40 m/s will be obtained. This is commonly known as an up and down test, as in Figure 15. The experimental v_{50} is calculated from Equation 11 below [11].

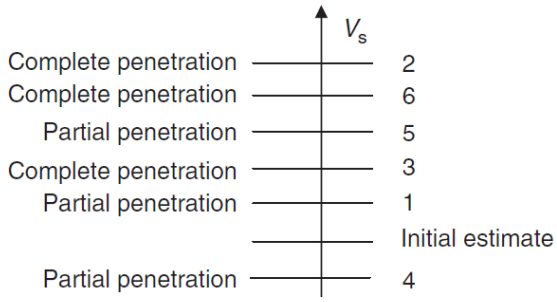

Figure 15. Up and down test procedure.

$$\boldsymbol{v_{50} = \frac{\sum_{i=1}^{6} Vi}{6}} \qquad \textbf{(11)}$$

The velocity below which a given projectile will not defeat a given target, v_i is also called the ballistic limit [11].

The following factors affect the limit velocity: material hardness, yaw at impact, projectile density, projectile nose shape, and length to the diameter ratio of the projectile, this has been experimental proven. In general for the material hardness, the harder target, the higher v_{50} becomes. When it comes to yaw at impact, the more yaw, the more chance for breakup or ricochet and the higher v_{50} will get. If the projectile density increases, the v_{50} will decrease. A blunter nose generally results in a higher v_{50}, but if the target is strongly overmatched, the nose shape has a negligible effect. The effect of the ratio between length and the diameter can go either way and depends mostly on the obliquity of the impact [11].

4. Method

This chapter explains the different test methods and materials that will be used during the study. The first part of the chapter, 4.1 to 4.3 informs about the materials properties, the different ammunitions that's will be used and the specimens. Then the rest of the chapter treats the different test methods.

4.1 Materials

The mechanical properties of Armox 500T and Armox 440T are shown below in Table 2.

Table 2. The mechanical properties of Armox.

	Thickness mm	Hardness HBW	Charpy-V -40˚C 10x10mm Joule	Yield Strength $R_{p,0.2}$ min MPa	Tensile Strength R_m MPa	Elongation A_5 min %	Elongation A_{50} min %
500T	3.0-80.0	480-540	25	1250	1450-1750	8	10
440T	4.0-30.0	420-480	35	1100	1250-1550	10	12

The chemical composition of Armox 500T and Armox 440T are shown below in Table 3.

Table 3. The chemical composition of Armox.

	C max %	Si max %	Mn max %	P max %	S max %	Cr max %	Ni max %	Mo max %	B max %
500T	0.32	0.4	1.2	0.015	0.010	1.0	1.8	0.7	0.005
440T	0.21	0.5	1.2	0.010	0.010	1.0	2.5	0.7	0.005

The bending testing will be limited to Armox 440T in thickness of 4, 6, 8 and 12 mm and also Armox 500T in thicknesses of 3, 4, 5, 6.5, 8 and 12 mm, those will all be performed in 90° bending angle in the bending test, as shown in Table 4.

Table 4. The different bending angles depend of the quality and dimension.

	Armox 440T 4mm	Armox 440T 6mm	Armox 440T 8mm	Armox 440T 12mm	Armox 500T 3mm	Armox 500T 4mm	Armox 500T 5mm	Armox 500T 6,5mm	Armox 500T 8mm	Armox 500T 12mm
30°			X	X				X		X
60°			X	X				X		X
90°	X	X	X	X	X	X	X	X	X	X

The ballistic testing will be limited to Armox 440T in thickness of 8 mm and 12 mm and Armox 500T in 6.5 mm and 8 mm and will also be performed in 30°, 60° and 90° bending angles as shown in Table 4.

4.2 Ammunition

The ammunition will be limited to a few ammunitions and threat levels, shown in Table 5. The limitations in the choice of ammunition has been made in order to the work's time limitation, therefore has the most requested ammunitions and threat levels been selected.

Table 5. The different ammunition for each quality and dimension.

	Armox 440T 8mm	Armox 440T 12mm	Armox 500T 6,5mm	Armox 500T 12mm
7,62x39 API BZ (STANAG 4569 Level 2)		X		X
FSP (STANAG 4569)		X		X
7,62x51 NATO Ball M80 (EN 1522 FB6)	X		X	
5,56x45 SS109/M855 (STANAG 4569 Level 1)	X		X	

4.3 Specimens

To develop the new bending recommendations a large amount of specimens were required to be produced. A standard sheet has the size of 2400x6000 mm, but Armox 500T 3 mm are supplied in 2000x4000 mm. Therefore 2 sheets were needed to get almost the same amount of specimens, and the cut layout did also differ. To produce usable specimens for the bending and ballistic tests, the sheets had to be cut down to specimens of a specific size of 600x300 mm. A cutout layout had been developed, as shown in Figure 16.

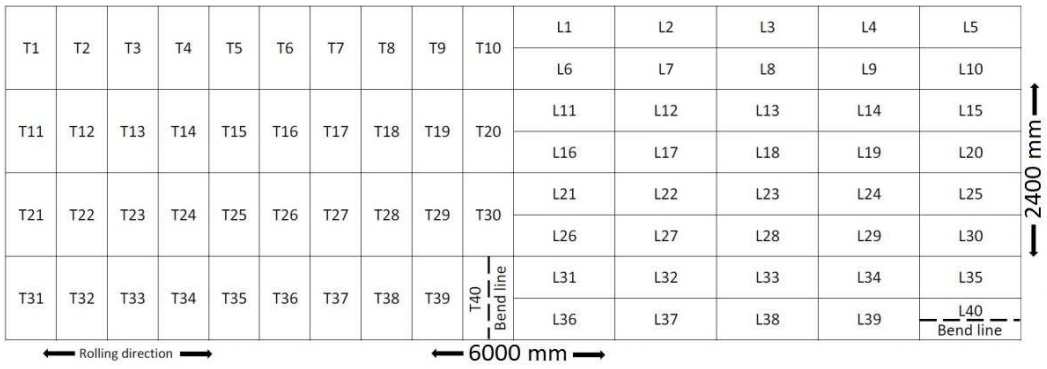

Figure 16. A schematic picture of the cutout layout for one sheet, and the name of the specimens, in addition to Armox 500T, t=3 mm.

The cutting was done at the workshop at SSAB Oxelösund.

4.4 Metallography

To attempt to explain the relationship between the bending radius and the ballistic resistance, a microstructure investigation was performed. In order to find a pattern in how the microstructure is affected by the bending radius, it was done by using previous bending specimens with a few different bending radii. The specimens to be investigated were two Armox 500T sheets, a 4 mm where the bending radius is 12 mm and a 6 mm where the radius is 19 mm.

From the bend sheets smaller pieces was cut out with a plasma cutter. Then the specimens were cut out again with a deformation-free precision cutter to avoid heat effect of the specimens and get an appropriate size for sample molding.

When all the specimens were cut out, they were casted into Bakelite. These Bakelite pucks were grinded and polished in a series of steps, the force and time was adapted for hard materials. Between every step the specimens was cleaned with ethanol in order to avoid abrasive particles followed to the subsequent step. Before and after each polishing step the specimens were cleaned in an ultrasonic bath to get as good surface as possible.

Then all the specimens were etched, two different etching methods was used, so there was two of each specimen. Initially one of each specimen was etched in a 3% Nital solution to obtain the microstructure. Then the nital etched specimens were ready to be studied in the microscope.

The other specimens were etched in picric acid to obtain the contours of the former austenite grain boundaries, in order to prove the degree of deformation and how the deformation has been affected by the bending. For this to be possible, the specimens were tempered in 520 ˚C for 16 h.

To increase the contrast on the sample surface the specimens was polished in 20 s with a 1 µm polishing disc and with ethanol as lubricant.

To study the specimens a light optical microscope (LOM) was used.

4.5 Microindentation hardness test

To evaluate the hardness of the bent material a hardness profile through the thickness was made by using the same two previous bending specimens as in Section 0, to try to understand the relationship between the bending radius and ballistic performance of the material. This was initially done at three locations in the bend to quickly get a result, as in Figure 17.

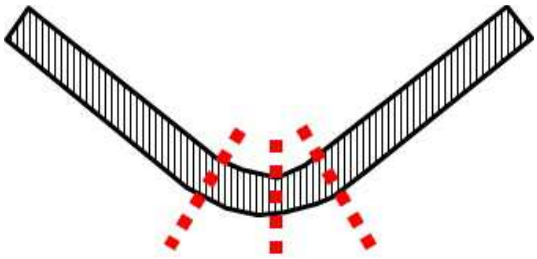

Figure 17. Schematic picture of the lines where the hardness profiles was made.

Then a hardness map was performed on one specimen, the Armox 500T with the thicknesses of r=4 mm and bending radius R=12 mm. Because of hardness mapping is more time consuming than hardness profiles, only one specimen was analyzed. Hardness mapping give a better and more reliable result, so the time is worth. Figure 18 shows a schematic picture of the mapping. A bunch of indents was made, and then the values were plotted to a colored surface map that describes the deformation in the bent material.

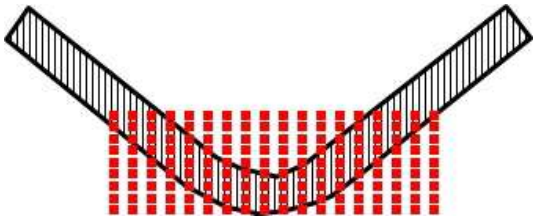

Figure 18. Schematic picture of the position of the hardness indents.

After studying the microstructure, the same specimens were used to evaluate the hardness of micro indentation hardness test, except for the tempered specimens. All in order to create a picture of how the material is affected by the bending process.

On each specimen three hardness profiles through the thickness were made, with the load of 500g. The first one was positioned in the center of the bend, and the other two was spaced ~5 mm from the center.

The hardness profiles consist of 30 micro hardness indentations. To do more indentations, will be more time consuming. Then the thickness of the specimens varies 4 and 6 mm, so the step length varies on each thickness. The number of indentations was limited to 30 because of the work time limitations and gave a fair balance against the resolution of the hardness profiles.

When the micro indentation hardness tester has done the indentations, then the user measured the indentations and it results in a table of the coordinates and hardness values. This data was then used to create a hardness profile through the thickness of the material.

To evaluate the hardness distribution over a bigger cross section area, a hardness mapping was done. There were 22 rows with 66 indentations in each,

with a 0.3 mm distance in both the X- and Y-direction, which gives a good resolution of the hardness.

The indentations in the bakelite have a much lower hardness value than the metal and are therefore easy to exclude. Then the hardness interval for the bakelite was excluded by setting the color of the interval to white on the map.

In Figure 19 below the hardness indentations distribution of the specimen are shown.

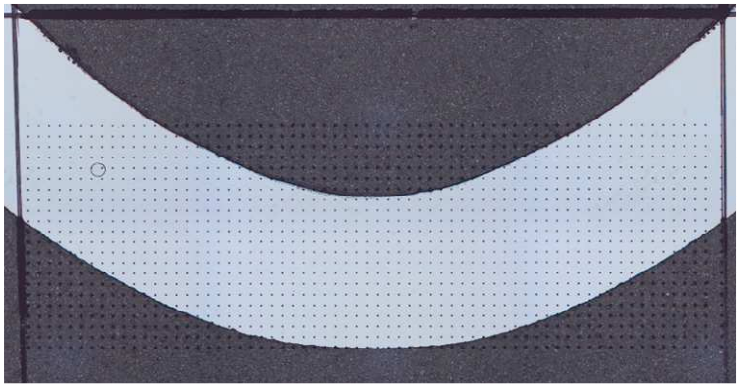

Figure 19. The distribution of hardness indentations on the bent specimen.

4.6 Bending of specimens

The bending was done at EM Eriksson and Forming laboratory at SSAB. EM Eriksson is a steel service center in Borlänge. Specimens thicker than 6 mm were done at EM Eriksson, specimens thinner than 6 mm were done at the Forming laboratory.

Half of the specimens were bent transverse and the other half was bent parallel with the rolling direction of the sheets. One full sized sheet (6000x2400 mm) for every quality and thickness were used to produce the specimens, in addition to Armox 500T 3 mm, two sheets was used (4000x2000 mm).

The current recommendations already specify a minimum ratio between the bending radius and material thickness. These ratios were the starting value for the test. EME did also bend specimens for the ballistic test; these were bended in 30˚, 60˚ and 90˚ and are marked with fat font in Table 6.

To the specimens to pass the bending test, no visible cracks can be catch by the eye. If a crack is catch by the eye, the specimen has not passed the test.

For the developing of the new recommendation the bending angle was 90˚ and with different ratio between the bending radius and the material thickness, as in Table 6, on the next page.

Table 6. The distribution of specimens for bending.

	Armox 440T 4mm		Armox 440T 6mm		Armox 440T 8mm		Armox 440T 12mm		Armox 500T 3mm		Armox 500T 4mm		Armox 500T 5mm		Armox 500T 6,5mm		Armox 500T 8mm		Armox 500T 12mm	
	T	P	T	P	T	P	T	P	T	P	T	P	T	P	T	P	T	P	T	P
	90° bending angle																			
R=8t															3	3				
R=7t			2	2	3	3									2	2	2	2		
R=6t			2	2	3	3									2	2	2	2		
R=5t	2	2	2	2	3	3	3	3	2	2	2	2	2	2	2	2	2	2	3	3
R=4t	2	2	2	2	3	3	3	3	2	2	2	2	2	2	2	2	2	2	3	3
R=3,5t	2	2	2	2	3	3	3	3	2	2	10	10	10	10	6	6	2	2	3	3
R=3t	10	9	10	10	3	3	6	6	10	10	2	2	4	2	3	3	7	7	7	7
R=2,5t	4	4	2	2	4	4	4	4	4	4					2	2	3	3	3	3
	60° bending angle																			
R=8t															2	2				
R=7t					2	2									1	1				
R=6t					2	2									2	2				
R=5t					2	2	2	2							2	2			2	2
R=4t					2	2	2	2							2	2			2	2
R=3t					2	2	2	2											2	2
	30° bending angle																			
R=8t															2	2				
R=7t															1	1				
R=6t					2	2									2	2				
R=5t					2	2	2	2							2	2			2	2
R=4t					2	2	2	2							2	2			2	2
R=3t					2	2														

T=Transverse, P=Parallel to rolling direction

4.7 Ballistic test of specimens

The shooting did take place at Åkers Krutbruk Protection AB in Åkers Styckebruk on their shooting range, the tests were very time consuming and took about 5 weeks to complete. The test is based on the use of the method v_{50}, which means that the ballistic limit where 50 % of six or more rounds with a maximum velocity spread of 40 m/s penetrates the armour, described in Section 3.6.4. Four different types of ammunition were tested corresponding to the standards, STANAG 4569 and EN 1522 and their matching threat levels Level 2 and FB6 to the used materials; where the thickness, radius and bending angle differs.

The test started with mounting the test plate at the shooting range. The first shot was fired to see which effect it has on the plate and the velocity of the projectile.

The first shot did only partially penetrate the plate. The second round started with filling up the cartridge with gunpowder to get more speed for the second shot. Then the second round completely penetrated the target. And so it went until three projectiles had completely penetrated and three projectiles partially penetrated the target plate. The maximum allowed velocity spread was 40 m/s between every round in the series. Then the average speed was then calculated for the series, and that is the v_{50}-value.

5. Results

5.1 Metallography

Armox is a martensitic steel, and the microstructure investigation resulted in two reference pictures of the microstructure, both undeformed. In Figure 16 below the microstructure of the undeformed Armox 500T is shown as a reference to the structures in Section 5.1.1 and 5.1.2.

Figure 20. Microstructure of undeformed Armox 500T, material with martensitic microstructure, 50x.

In an attempt to see the deformation in the materials, the material was tempered and etched in Picric acid to obtain the contours of the former austenitic grain boundaries. In Figure 21 below the microstructure of tempered and undeformed material is shown as a reference to the structures in Section 0 and 5.1.4.

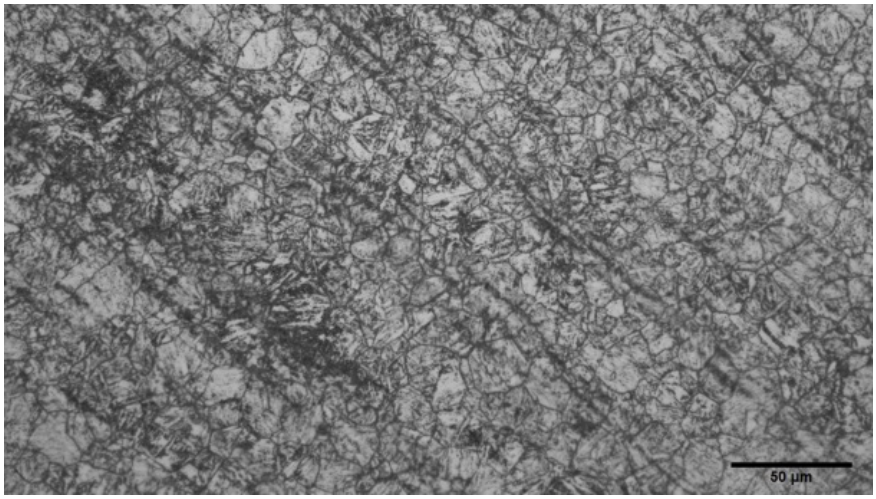

Figure 21. Microstructure of undeformed and tempered Armox 500T material with martensitic microstructure with the former austenite grains visible, 50x.

5.1.1 Armox 500T 4 mm radius 12 mm

The microstructure investigation resulted in pictures of the microstructure of the two thicknesses, both Armox 500T, first a 4 mm, with a bending radius of 12 mm, and then a 6.5 mm with a bending radius of 19.5 mm.

The pictures below show the microstructure from three locations in the middle of the bend. In Figure 22 the microstructure of the convex side of the bend is shown, the in Figure 23, the microstructure of the neutral plane is shown. Then the microstructure of the concave side of the bend is shown in Figure 24.

Figure 22. Microstructure on the convex side of the bend, Armox 500T, plate thickness t=4 mm, bending radius R=12 mm, material with martensitic microstructure, 50x.

Figure 23. Microstructure of the neutral plane, Armox 500T, plate thickness t=4 mm, bending radius R=12 mm, material with martensitic microstructure, 50x.

Figure 24. Microstructure on the concave side of the bend, Armox 500T, plate thickness t=4 mm, punch radius R=12 mm, material with martensitic microstructure, 50x.

5.1.2 Armox 500T 6.5 mm radius 19.5 mm

The pictures below shows the microstructure from three locations in the middle of the. In Figure 25 the microstructure of the convex side of the bend is shown, and then in Figure 26, the microstructure of the neutral plane is shown. Then microstructure of the concave side of the bend is shown in Figure 27.

Figure 25. Microstructure on the convex side of the bend, Armox 500T, plate thickness t=6.5 mm, punch radius R=19.5 mm, material with martensitic microstructure, 50x.

Figure 26. Microstructure of the neutral plane, Armox 500T, plate thickness t=6.5 mm, bending radius R=19.5 mm, material with martensitic microstructure, 50x.

Figure 27. Microstructure on the concave side of the bend, Armox 500T, thickness t=6.5 mm, bending radius R=19.5 mm, material with martensitic microstructure, 50x.

5.1.3 Tempered Armox 500T 4 mm radius 12 mm

The pictures below shows the former austenitic grains in the convex side, neutral plane and concave side of the bend, in attempt to see the deformation.

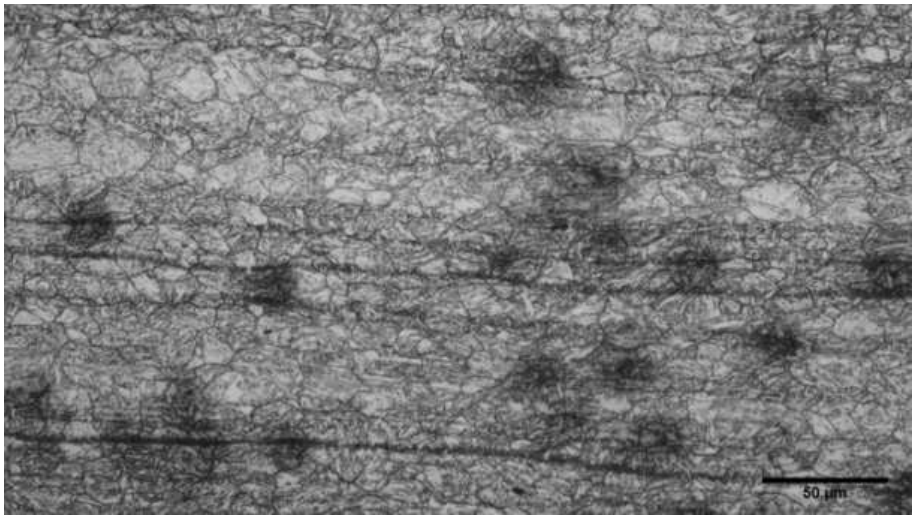

Figure 28. Former austenitic grains on the convex side of the bend, Armox 500T, plate thickness t=4 mm, bending radius R=12 mm, with martensitic microstructure with the former austenite grains visible, 50x.

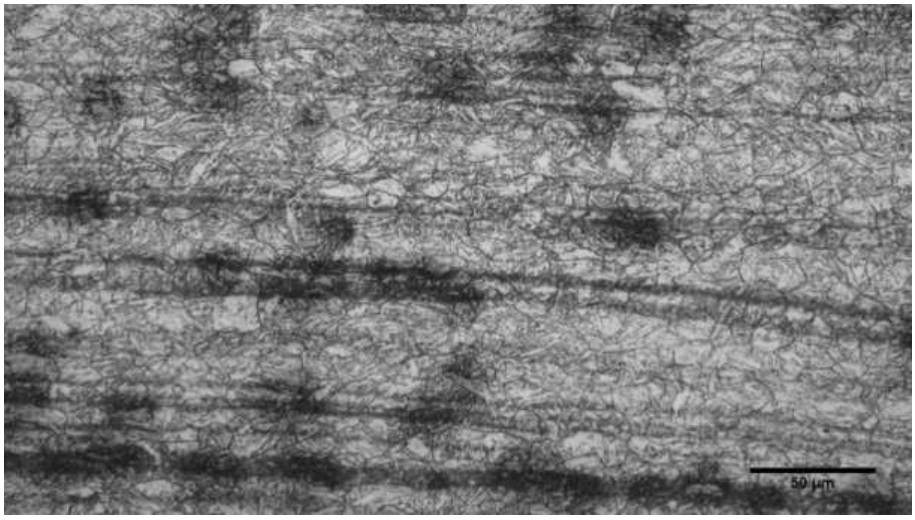

Figure 29. Former austenitic grains in the neutral plane, Armox 500T, thickness t=4 mm, bending radius 12 mm, with martensitic microstructure with the former austenite grains visible, 50x.

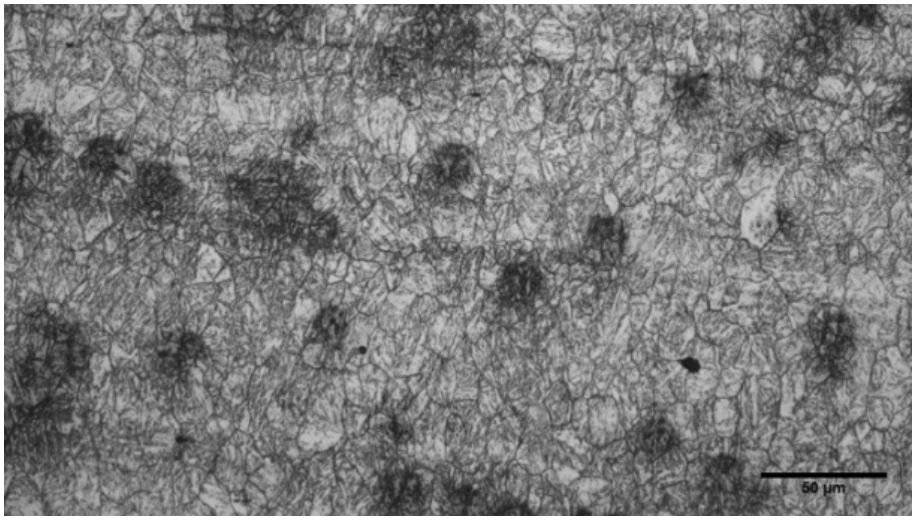

Figure 30. Former austenitic grains on the concave side of the bend, Armox 500T, thickness t=4 mm, bending radius 12 mm, with martensitic microstructure with the former austenite grains visible, 50x.

5.1.4 Tempered Armox 500T 6.5 mm radius 19.5 mm

The pictures below shows the former austenitic grains in the convex side, neutral plane and concave side of the bend, in attempt to see the deformation.

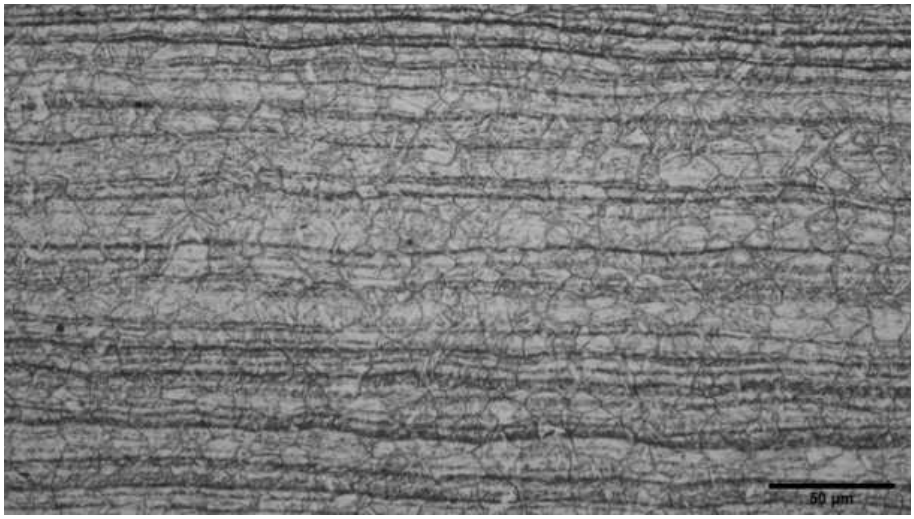

Figure 31. Former austenitic grains on the convex side of the bend, Armox, thickness t=6.5 mm, bending radius 19.5 mm, with martensitic microstructure with the former austenite grains visible.

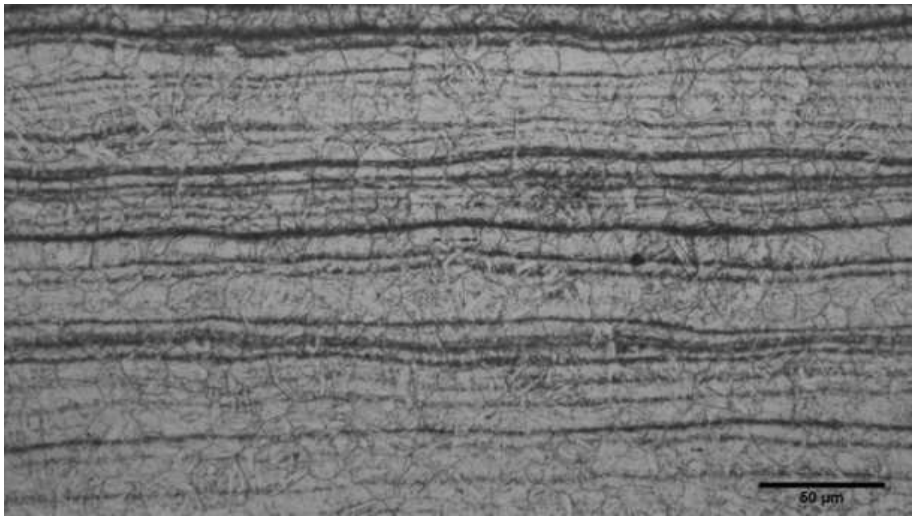

Figure 32. Former austenitic grains on the neutral plane, Armox , thickness t=6.5 mm, bending radius 19.5 mm, with martensitic microstructure with the former austenite grains visible, 50x.

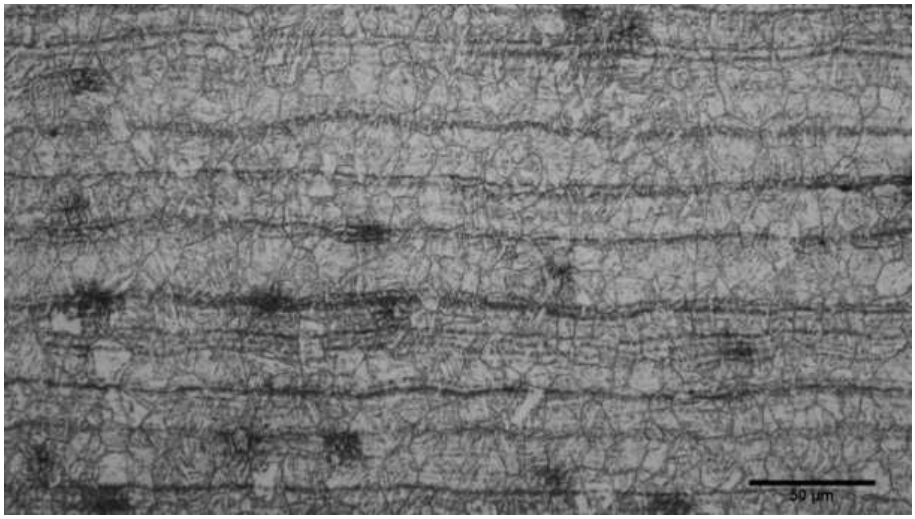

Figure 33. Former austenitic grains on the concave side of the bend, Armox 500T, thickness t=6.5 mm, bending radius 19.5 mm, with martensitic microstructure with the former austenite grains visible, 50x.

5.2 Microindentation hardness test

The micro indentation hardness test resulted in two hardness profiles, one for each thickness. In Figure 34 below the hardness profile for Armox 500T 4 *mm*, with a radius of 12 mm are shown. Because of decarburization, the hardness is lower closest to the surfaces. Distance zero represents the thickness thru the bend, from the concave side to the convex side of the bend. The left mark on Figure 17, representing the left curve, the middle mark representing the middle curve and the right mark the right curve.

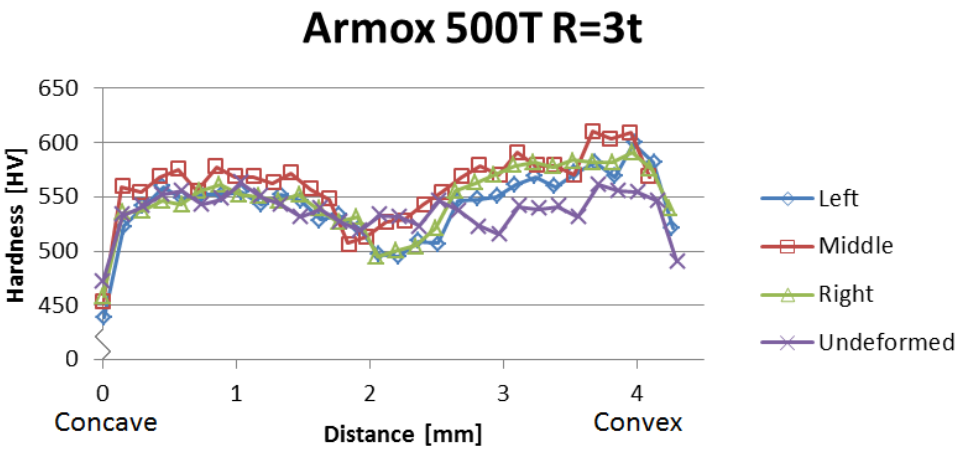

Figure 34. The hardness profile through the thickness of Armox 500T, bending radius R=12 mm, thickness t=4 mm.

In Figure 35 below the hardness profile for Armox 500T 6.5 mm, with a bending radius of 19.5 mm are shown.

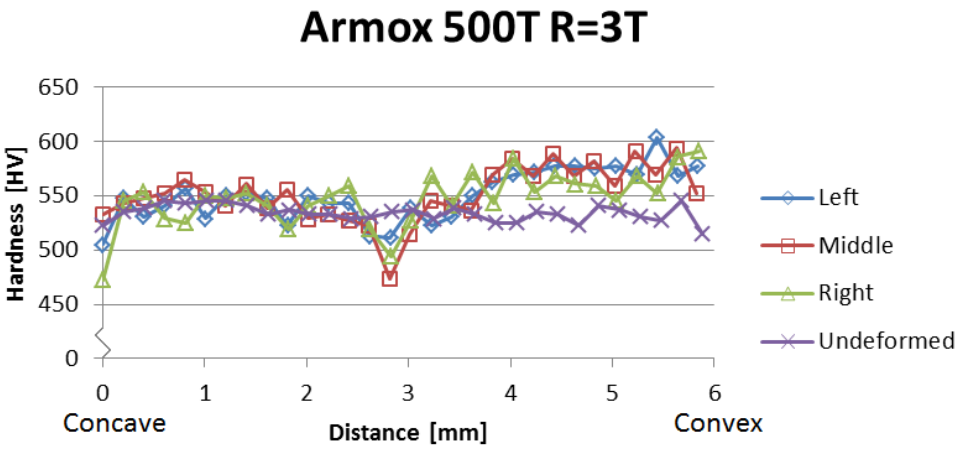

Figure 35. The hardness profile through the thickness of Armox 500T, bending radius R=19.5 mm, thickness t=6.5 mm.

The hardness mapping of Armox 500T, 4 *mm* with radius of 12 *mm* resulted in the plot below in Figure 36. To draw up the hardness map of the specimen, 1452 indentations were made, as the schematic picture in Figure 18, and the resulting surface on the specimen in Figure 19. Each color represents a hardness interval, the warmer color of a point, the harder it is.

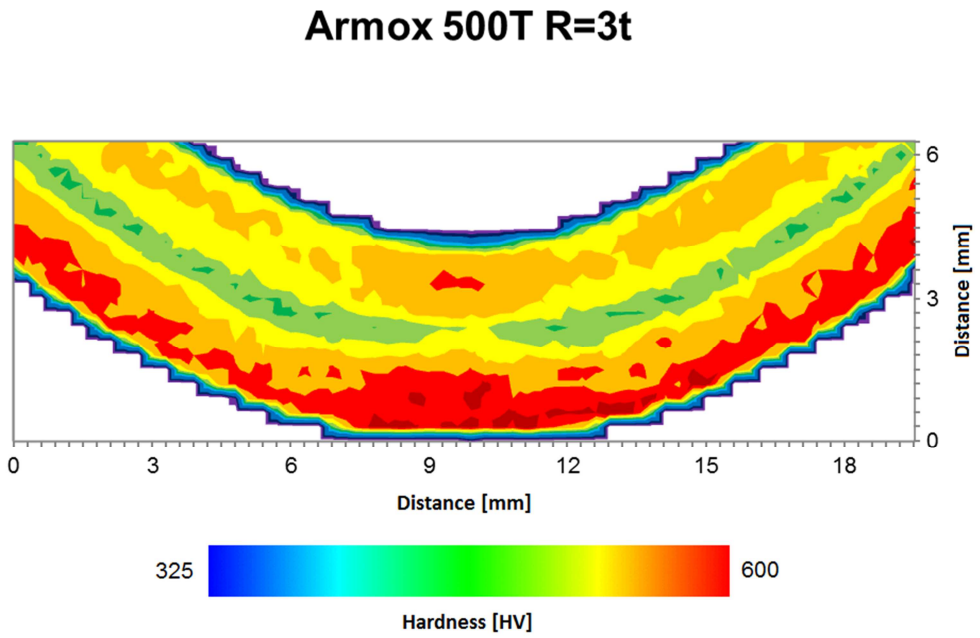

Figure 36. The hardness mapping of Armox 500T, 4 *mm*, with radius 12 *mm*, 1452 indentations.

5.3 Bending of specimens

The result from the bending tests is display below in Table 7. Numbers in green passed the test, when numbers in red and italic style did not pass the test, cracks was catch by eye.

Table 7. The results from the bending tests of Armox.

	Armox 440T 4mm		Armox 440T 6mm		Armox 440T 8mm		Armox 440T 12mm		Armox 500T 3mm		Armox 500T 4mm		Armox 500T 5mm		Armox 500T 6,5mm		Armox 500T 8mm		Armox 500T 12mm	
	T	P	T	P	T	P	T	P	T	P	T	P	T	P	T	P	T	P	T	P
90° bending angle																				
R=8t															3	3				
R=7t			2	2	3	3									2	2	2	2		
R=6t			2	2	3	3									2	2	2	2		
R=5t	2	2	2	2	3	3	3	3	2	2	2	2	2	2	2	2	2	2	3	3
R=4t	2	2	2	2	3	3	3	3	2	2	2	2	2	2	2	2	2	2	3	3
R=3,5t	2	2	2	2	3	3	3	3	2	2	10	10	10	10	6	6	2	2	3	3
R=3t	10	9	10	10	3	3	6	6	4	4	*2*	*2*	4	*2*	3	*3*	7	7	7	7
R=2,5t	*4*	*4*	*2*	*2*	4	4	*4*	*4*	*4*	*4*					*2*	*2*	*3*	*3*	3	3
60° bending angle																				
R=8t															2	2				
R=7t					2	2									1	1				
R=6t					2	2									2	2				
R=5t					2	2	2	2							2	2			2	2
R=4t					2	2	2	2							2	2			2	2
R=3t					2	2	2	2											2	2
30° bending angle																				
R=8t															2	2				
R=7t															1	1				
R=6t					2	2									2	2				
R=5t					2	2	2	2							2	2			2	2
R=4t					2	2	2	2							2	2			2	2
R=3t					2	2														

T=Transverse, P=Parallel to rolling direction

5.4 Ballistic test of specimens

The ballistic testing resulted in a protocol for every performed v_{50}-test. These protocols were summed into an Excel-document, and then a graph was created for every combination of thickness, quality and ammunition. These graphs are shown below in Section 5.4.1 to Section 5.4.4. The reference targets were made by v_{50}-tests performed at undeformed target plates.

5.4.1 Armox 500T 6.5 mm

The results from the ballistic testing are presented below in Figure 37 and Figure 38. Figure 37 presents the results of 5.56x45 SS109 and Figure 38 the

results of 7.62x51 NATO Ball. The lines are the references v_{50}´s, the result from the same ammunition and undeformed material. The reason for this is to show how undeformed target material performs.

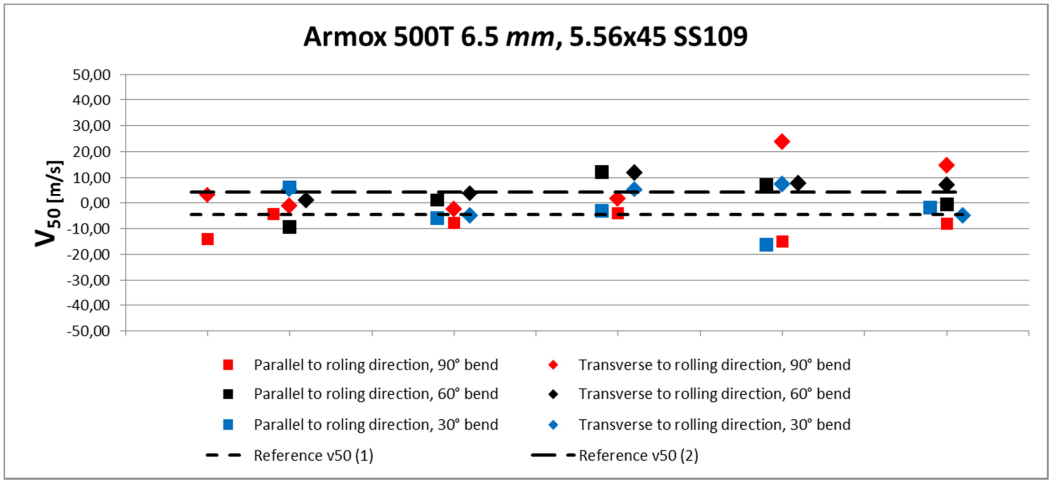

Figure 37. Results from the ballistic testing of Armox 500T, thickness t=6.5 mm, 5.56x45 SS109.

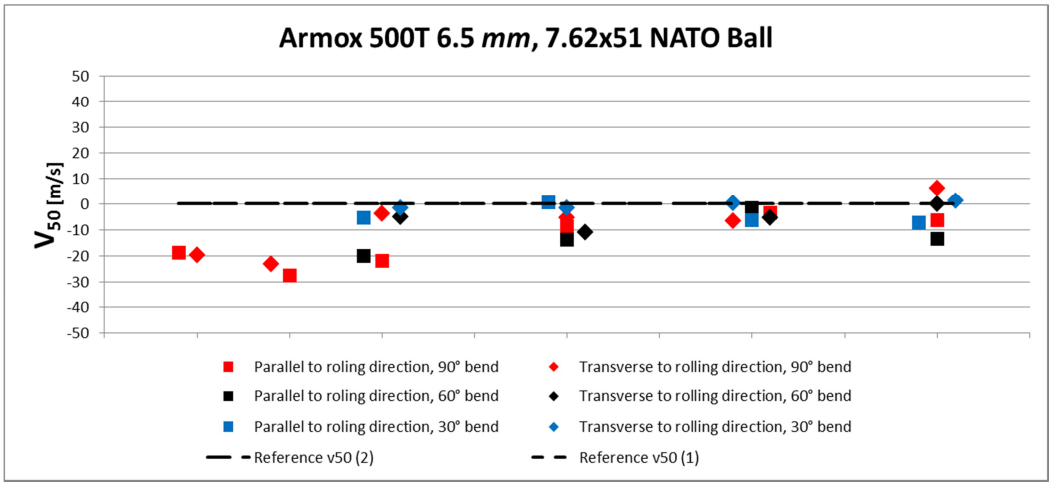

Figure 38. Results from the ballistic testing of Armox 500T, thickness t= 6.5 mm, 7.62x51 NATO Ball.

5.4.2 Armox 440T 8 mm

The results from the ballistic testing are presented below in Figure 39 and Figure 40. Figure 39 presents the results of 5.56x45 SS109 and Figure 40 the results of 7.62x51 NATO Ball. The lines are the references v_{50}´s, the result from the same ammunition and undeformed material. The reason for this is to show how undeformed target material performs.

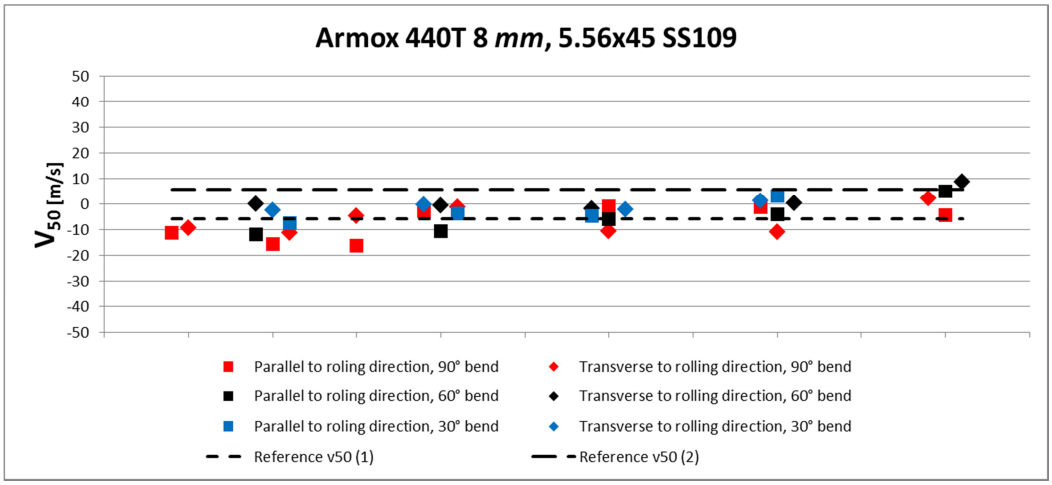

Figure 39. Results from the ballistic testing of Armox 440T, thickness t= 8 mm, 5.56x45 SS109.

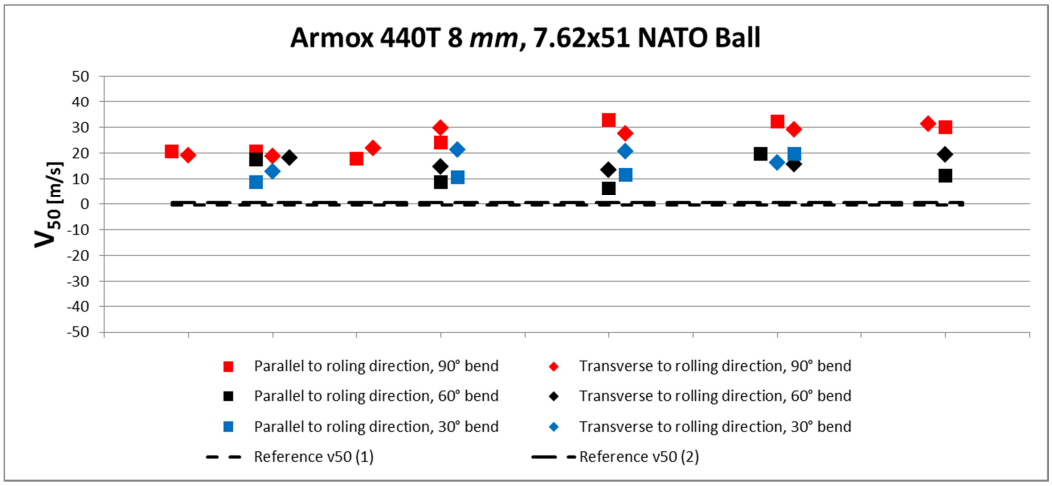

Figure 40. Results from the ballistic testing of Armox 440T, thickness t= 8 mm, 7,62x51 NATO Ball.

5.4.3 Armox 500T 12 mm

The results from the ballistic testing at Åkers Krutbruk Protection AB are presented below in Figure 41. The test of 7,62x39 API BZ on Armox 500T 12 mm failed, because it was not possible to accomplish complete penetration. Figure 41 shows the results of 20 mm FSP. The lines are the references v_{50}´s, the result from the same ammunition and undeformed material. The reason for this is to show how undeformed target material performs.

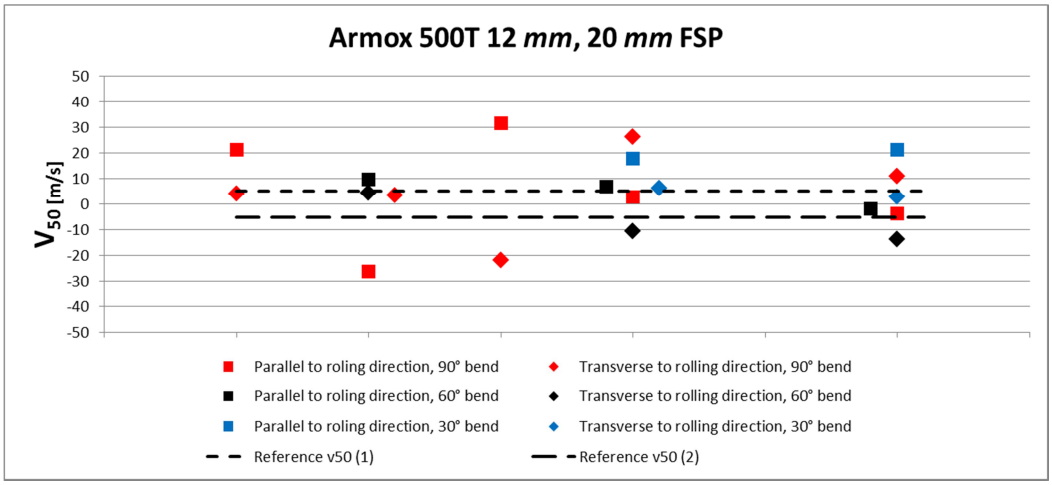

Figure 41. Results from the ballistic testing of Armox 500T, thickness t=12 mm, 20 mm FSP.

5.4.4 Armox 440T 12 mm

The results from the ballistic testing are presented below in Figure 42 and Figure 43. Figure 42 presents the results of 7,62x39 API BZ and Figure 43 the results of 20 mm FSP. The lines are the references v_{50}´s, the result from the same ammunition and undeformed material. The reason for this is to show how undeformed target material performs.

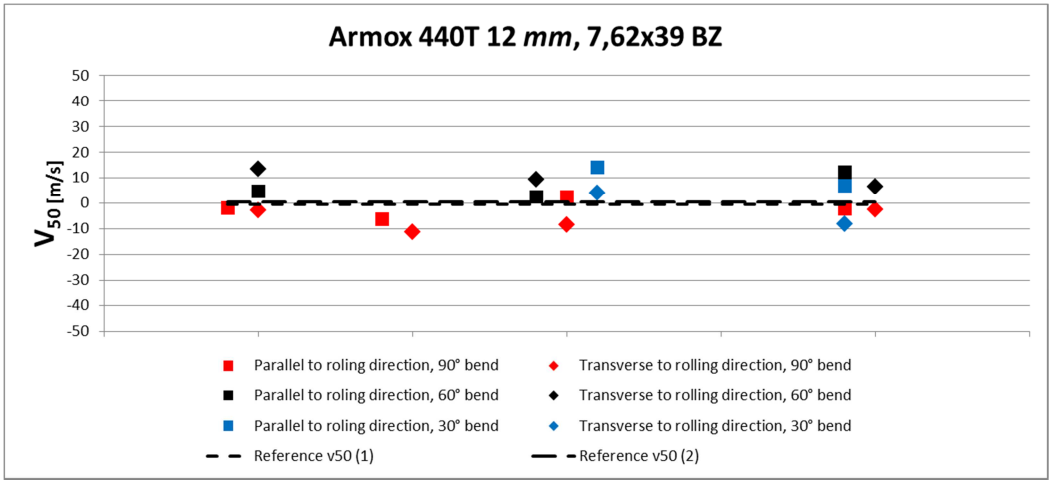

Figure 42. Results from the ballistic testing of Armox 440T, thickness t=12 mm, 7,62x39 API BZ.

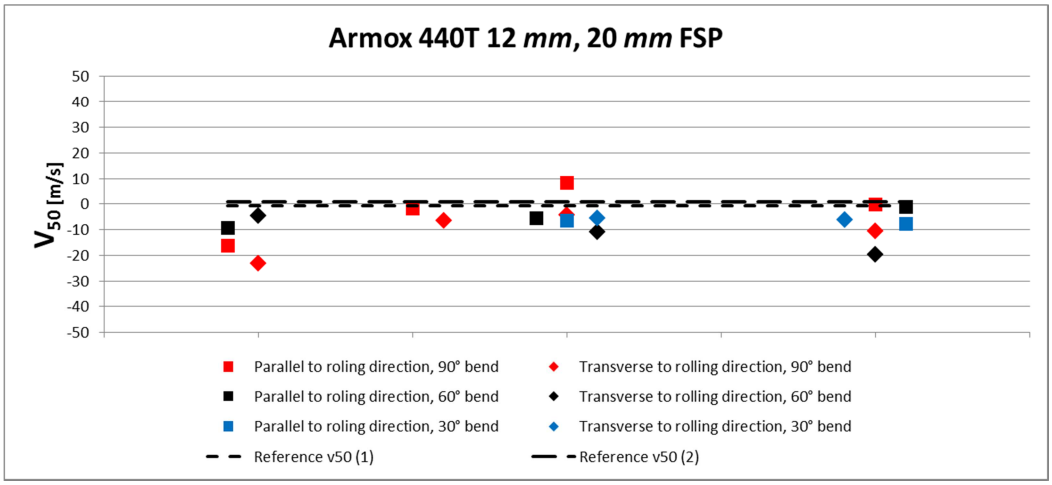

Figure 43. Results from the ballistic testing of Armox 440T, thickness t=12 mm, 20 mm FSP.

6. Discussion

All the results have been analyzed to find differences and causes to why the bending should affect the ballistic properties. Each experiment and its result are discussed below in Section 6.1 to Section 6.4.

6.1 Metallography

These tests were made with the intention to see how the microstructures change after bending. To see if the expected changes in the microstructures will have an effect on the later ballistic testing.

It was first expected to get changes in the microstructure, to get stretched grains on the convex side of the bend, because of the tensile stresses, and on the same time get compressive stresses on the concave side, resulting in compressed grains [21].

After analyzing the different specimens, with the different punch radius and material thickness ratios, in the LOM. It was not possible to see any changes of the microstructure of the bent material. By this time the specimens were only etched in 3% Nital solution, which only exposed the martensitic microstructure, which makes it difficult to see any signs of deformation.

The next step was to try to expose the former austenite grain boundaries. After help from Jonas Östberg at the Metallography Department, the specimens were etched in picric acid, which exposed the former austenite grain boundaries. Unfortunately, it was still not possible to see any deformation to the grains [22].

Professor Göran Engberg was then contacted to get any comments about the result; his comment was that it was not expected to see any signs of deformation in the martensitic material [23].

Then a meeting was setup with Dr. Jenny Fritz at SSAB´s R&D department to discuss the deformation mechanism for martensitic steels. The meeting resulted in the knowledge that the deformation mechanism for martensitic steel is not fully established, only some theories of what happens in the microstructure during deformation. Therefore the investigation of the microstructure ended [24].

6.2 Microindentation hardness test

To know what happens to the material when it is deformed, another method was needed to identify the effect bending has on the material, which could affect the ballistic properties.

It was decided to do hardness profiles through the thickness, at three points on each specimen with different ratios between the thicknesses and the punch radius. The profiles confirmed the theory that the hardness will increase on the convex side of the bend because of the work hardening, also the concave side of the bend get an increase in hardness, but not as much as the convex side. The neutral axis stayed unaffected as the theory says. The result was the same on both specimens [9].

After a discussion about the results with Jonas Östberg, he introduced microindentation hardness mapping, which give the whole picture of the effect of deformation of the bent material [22].

After the investigation was made, the result was compared to the earlier made hardness profiles, the result matched between them. The question was still to find out which effect this will have on the ballistic properties of Armox.

If the hardness increases with the amount of deformation, the ductility should reduce, then it is possible that a saddle point exists. When it is possible that the increase of hardness is positive and the ductility is high enough to absorb the energy from the ballistic projectile, means that the bending have a positive effect on the ballistic properties until the ductility decreases too much to absorb the energy of the projectile.

6.3 Bending of specimens

To leave bending recommendations at SSAB, the internal policy says that the total tested bend length need to be 5000 mm. The specimen size was therefore determined to be 600 mm x 300 mm. The press brake required the specimens to be a minimum 300 mm in depth to be able to bend them.

The test was based on the earlier recommendations, also lower ratios between the punch radius and thickness was tested to develop the recommendations further. The major part of the test was intended to find the smallest ratio, and therefore the biggest amount of specimens was tested on the lower ratios.

The outcome of the test was very successful and no problems during the test were encountered. The results from the test are really good comparing to the older bending recommendation.

Some of the thicknesses that were tested failed with the lowest ratios in the bending test. For some thicknesses and grades, the result differs between the parallel and transversal specimens.

In the theory, the bendability is better for the transverse specimens than the parallel to the rolling direction, due to the anisotropy after rolling [9].

The results for Armox 500T; 5 and 6.5 mm complies with the theory, due to the anisotropy of the rolled material. Unfortunately, it only appears on the results for Armox 500T; 5 and 6.5 mm in Table 7. Perhaps it is because the lower limit is just above; for those that failed at the same ratio for both parallel and transversal, or below; for those that succeed with all the tested ratios.

The things that could have been improved in the test would have been to lubricate the die-rolls between every bending procedure and use cleaned specimens.

6.4 Ballistic test of specimens

The results from the ballistic testing do not match with the expectations SSAB had before the test. The expectations were that the ballistic performance would deteriorate progressively with lower ratio between the thickness and the punch radius; this was based on information from earlier tests [4].

According to the results, the bending does not significantly influence the ballistic properties for the tested Armox material and ammunition combinations. This may due to the increase of hardness in the material during bending, without losing too much ability to absorb energy from the projectile, as mentioned in the end of Section 6.2. The differences between the v50-values for the deformed and undeformed specimens are quite small; in percentage comparison is under five percent difference.

The testing was very time consuming, the spread of the projectiles in both velocity and hit accuracy was the major problems during the test.

7. Proposals to further studies

Further studies can be done in this subject; due to it is a large and relatively unexplored subject. There are many different aspects that may influence the results and therefore it is suitable for further investigation. Here are some suggestions for further investigation;

- Analyze several ratios between the punch radius and the thickness with hardness mapping.
- Analyze the material with SEM/EBSD on an undeformed specimen and a bended specimen to see any motion in the materials texture.
- Analyze several specimens, several thicknesses, qualities and ammunitions. Due to the complexity in ballistics and the need to test each system individually, to be able to draw some conclusions.

8. Conclusion

The purpose of this thesis was to investigate how bending affects the ballistic properties of Armox. The result from the testing shows that the bending does not have any significantly effect on the ballistic properties on these tested combinations. Relevant conclusions that can be identified are;

- The ability to release new and better bending recommendations for Armox 440T and 500T.
- The bending does not significantly influence the ballistic properties for the tested materials and ammunitions.
- It is possible that the bending affects the ballistic properties of the material, increases the hardness, which is positive to the ballistics, and also decreases the ability to absorb energy during bending, which is negative. Unfortunately, the limit when the ability to absorb energy becomes too low was not found during the testing.
- Further investigation need to be done to confirm these theories.

9. Acknowledgements

I would like to express my deepest appreciation to all those who provided me the possibility to complete this thesis. A special gratitude I give to my supervisor, B.S. Oscar Ivarsson at SSAB Protection & Tooling, whose contribution in stimulating suggestions and encouragement helped me to finish my project.

Furthermore I would also like to acknowledge with much appreciation the crucial role of the staff of SSAB EMEA, who gave the permission to use all required equipment and the necessary materials to complete the thesis. Specifically, M.Sc. Jonas Östberg at SSAB's Metallography department, for his support and invaluable guidance in the laboratory.

I would also like to extend a special thanks to my supervisor at Dalarna University, Doc. Lars Karlsson, for his support, commitment and also for good guidance in this thesis.

Then I want to thank Åkers Krutbruk Protection AB for the good cooperation with the ballistic testing, especially Fredrik Bratt at Åkers who helped me at that point.

10. References

[1] SSAB EMEA, "The steel you want between you and the risk," 2014. [Online]. Available: http://www.ssab.com/Global/ARMOX/. [Accessed 01 06 2014].

[2] "SSAB," [Online]. Available: http://www.ssab.com. [Accessed 05 02 2014].

[3] SSAB EMEA, "The steel book," 2012. [Online]. Available: http://www.ssab.com/Global/SSAB/Brochures/. [Accessed 01 06 2014].

[4] O. Ivarsson, Interviewee, *Ballistic Engineer*. [Interview]. 17 02 2014.

[5] SSAB EMEA, "Armox workshop recommendations," [Online]. Available: http://www.ssab.com/Global/ARMOX/Brochures/en/. [Accessed 01 06 2014].

[6] P. Jönsson, "KTH," Framställningsmetoder metaller, [Online]. Available: http://www.met.kth.se/utbildning/4H1063/Lect10a-4H1063-metals.pdf. [Accessed 03 02 2014].

[7] B. Bergman and M. Selleby, Materiallära för materialdesign, KTH, 2009.

[8] SSAB EMEA AB, Plåthandboken, Nyköping, 2010.

[9] SSAB Tunnplåt, Formningshandboken, 1998.

[10] ASM Handbook, Bending of Sheet Metal, Metalworking: Sheet Forming, Vol 14B, 2006.

[11] D. Carlucci and S. Jacobson, "Ballistics, theory and design of guns and ammunition," Taylor & Francis Group, 2007.

[12] NATO, "Standardization Agreement," 2004.

[13] CEN, "Windows, doors, shutters and blinds - Bullet resistance - requirements and classification," 1998.

[14] VPAM, "General basis for ballistic material, construction and product tests," 2009.

[15] CEN, "Windows, doors, shutters and blinds - Bullet resistance - Test method.," 1998.

[16] F. C. Barnes, Cartridges of the World, 12th Edition, 2009.

[17] U.S. Department of Defense, "DETAIL SPECIFICATION, PROJECTILE, CALIBERS .22, .30, .50, AND 20MM FRAGMENT-SIMULATING," 2006.

[18] Transeco Bremen, "Material | Transeco Bremen," [Online]. Available: http://www.transeco-bremen.de/ballistic/material/. [Accessed 18 02 2014].

[19] U.S. Department of Defense, "V50 Ballistic test for armor," 1997.

[20] NIJ, "Ballistic Resistant Protective Materials," 1985.

[21] S. Jonsson, Mechanical Properties of Metals and Dislocation Theory from an Engineer's Perspective, 2008.

[22] J. Östberg, Interviewee, *M.Sc.*. [Interview]. 2014.

[23] G. Engberg, Interviewee, *Professor.* [Interview]. 13 03 2014.

[24] J. Fritz, Interviewee, *Doctor.* [Interview]. 10 04 2014.